Weber and Lehmkuhl
Environmental Sciences Europe (2024) 36:109
https://doi.org/10.1186/s12302-024-00926-5

Environmental Sciences Europe

RESEARCH

Open Access

Mixed response of trace element concentrations in fluvial sediments to a flash flood in a former mining area

Alexandra Weber[1*] and Frank Lehmkuhl[1]

Abstract

Background Floods, especially flash floods, are the major transporting agent for fluvial sediments, whose pollution is a global concern. As floods result in the dispersion of and exposure to these sediments, a profound understanding of sedimentary dynamics during flood events and the related pollutant dispersion is of relevance. However, the characteristics of extreme flood events concerning pollutant dynamics are insufficiently known so far.

Results In a Central European catchment impacted by intense industrial activities and former mining, over the course of five years, we surveyed six high-discharge events, five of them approx. bankfull discharge and one major flash flood event, supplemented by sampling of bank sediments. Fluvial sediments were analyzed for elemental composition by X-Ray fluorescence and for grain size distribution of the fine faction by laser diffraction. By applying a local enrichment factor, trace metal(loid) signatures in these sample sets were compared. Furthermore, Positive Matrix Factorization was used to investigate the trace metal(loid)s' sources.

The sediments deposited by minor flooding had continual trace metal(loid) signatures. However, for the extreme event, significant divergencies arose and persisted for the following years: The enrichment of anthropogenically influenced elements increased, with a slowly decreasing trend in the subsequent two years. Naturally dominated metal(oid)s decrease in enrichment without indicating a return to original levels. In contrast, other elements were insensitive to the extreme event. Positive Matrix Factorization identified anthropogenic influences in elements originating from copper and lead processing and mining activities. Furthermore, bed sediments and a natural background factor were found to dominate the non-anthropogenically influenced metal(loid)s.

Conclusions In between extreme events, winnowing processes slowly alter the elemental composition of bed sediments. The depletion of such sediments due to the flash flood proves catchment-wide flushing, which induces a natural resetting of the geochemical signals. This ability to renew is an integral part of resilience in fluvial systems. This mechanism is disturbed by industrial activities in floodplains. The exceptional flooding reaches infrastructure that is assumed to be safe and, therefore, unprotected. These additional sources can shift flood sediments' trace metal(loid) signature, which has a long-lasting impact on the catchment sediments. However, the modifications depend on the flooding extent, possible emitters, and protection measures.

Keywords Flood-related trace element dynamics, Contamination, Trace metals, Mining area, Source identification, PMF, Heavy metals, July 2021 flood, Flash flood, Fluvial sediments

*Correspondence:
Alexandra Weber
alexandra.weber@geo.rwth-aachen.de
[1] Department of Geography, RWTH Aachen University, Wüllnerstr. 5B, 52062 Aachen, Germany

Introduction

Mining-related pollution of fluvial systems and related health issues are a global concern [1–9]. Trace metal(loid)s are of particular relevance as they are persistent, non-biodegradable, and, therefore, accumulate along the food chain while sometimes being toxic at already small concentrations [10–13]. The exceptional longevity of mining-induced trace metal(loid) contamination further aggravates the situation [3].

Since more than 90% of trace metal(loid)s are transported as particulate matter [14, 15], sediments must be addressed to understand the dynamics and the fate of trace metal(loid)s [16]. Flood events can induce vigorous sediment mobilization in relatively short periods [17, 18]. Notwithstanding the prognosis of rising frequencies and magnitudes of flood events due to climate change [19, 20], a growing part of the human population lives in flood-prone areas [21–24]. Yet, despite being relevant to millions of people, the risks arising from flood sediments are often neglected [25].

No simple, straightforward correlation exists between trace element[1] concentration and discharge or sediment load [26–30]. In the first stages of flooding, i.e., during the rising limb, unconsolidated fine sediments get eroded, leading to quickly rising concentrations of suspended sediments that reflect the contamination status of bed and channel sediments [14]. However, they are mostly washed out of the catchment, as floodplain deposition occurs during receding waters [14]. During the following stages, the situation depends on the sediments eroded: while some studies report high discharges leading to intensified input of pollutants into the fluvial system (e.g., by erosion of pollution sinks) and, in turn, to enhanced concentrations of contaminants in flood sediments [4, 14, 15, 31–34], others provide evidence for the limited influence of flooding on pollutant levels [35, 36] or even decreasing of pollutant concentration due to flushing of the catchment [37, 38] or suggest dilution with 'clean' sediments [26, 30, 39–42]. Depending on the pollution intensity and distribution within the catchment, there is a variable discharge threshold above which additional pollutant sources outweigh the dilution effect [43]. On the other hand, flooding can induce the exhaustion of pollution sources. A further influence on the trace element concentrations arises from the area of deposition [30, 43]. Hence, the impact of extreme flood events on the dynamics of sediment-bound pollution is highly catchment-specific and depends on the initial state of the catchment's sediments prior to the flooding.

[1] To simplify matters, we use the term 'trace elements'; however, we only investigated trace metals and metalloids.

The evaluation of the influence of flooding on trace element concentrations is further complicated by the general complexity inherent in working with geochemical data [44–46]. The observed concentration of trace elements depends on the sediment's characteristics (e.g., grain size distribution and organic matter content) and, hence, cannot be interpreted directly but must be thoroughly prepared for analysis [17, 46–49]. Therefore, the direct interpretation of concentration measurements cannot provide meaningful results [47, 50–52]. Instead, combining traditional approaches of trace element evaluation, like classic enrichment factors, with methods relying on robust statistics seems favorable, as Famera et al. [53] suggested. Efficient mitigation of the risks arising from contaminated flood sediments requires a solid understanding of the interplay of influencing factors to provide a mandatory long-term perspective [54]. Hence, a thorough analysis of the main sources of possible risk elements is inevitable. A widely used tool is factor analysis (FA), which identifies influencing factors by relying on statistically evident relations between measurands [55, 56]. Among them, Positive Matrix Factorization (PMF) has proven to be especially useful [57–65]. Developed by Paatero and Tapper in 1994 [66], it was initially mainly used to investigate atmospheric pollutants [60, 67–76]. However, in recent years, it has been successfully applied to a variety of fields like groundwater [77], streamwater [78], rainwater [79], provenance analysis [80], and especially trace elements in sediments [62, 81–87]. PMF, which can be implemented relying on robust statistics [58, 88, 89], does not require any a priori knowledge of the emission profiles [56, 82].

In this study, we attempt to improve the understanding of how extreme flash flood events differ from regular flooding events regarding trace element dynamics. To this end, we compare trace element enrichment in flood sediments of flood events of differing magnitude in a Central European catchment severely impacted by historical mining and industrial activities. FA employing PMF provides further insight into the sources of trace elements and sediment dynamics. This approach combines the rather 'traditional' method of enrichment assessment with a robust statistical analysis.

Thereby, we address the following hypothesis:

1. The trace element signature in fluvial deposits is discharge-dependent. This implies similar geochemical profiles for regularly reoccurring high-discharge events (bankfull discharge or events that induce minor flooding of the floodplains at most) and deviations from that trace element inventory for extreme events. We assume these divergences to be element-dependent.

2. The impact of the extreme event on the channel sediment's geochemistry is longer-lasting.
3. PMF is a suitable tool for investigating complex sedimentary systems affected by an unknown number of emission sources with not entirely homogenous emission profiles.

Methods

Study area—the Inde catchment

The Inde River catchment, 344 km^2 in area, is located in western Europe in Belgium and Germany. The perennial river's source is in the medium-range mountains of the northern Eifel. After 30 km, it enters the Lower Rhine Embayment before watering into the Rur River (Fig. 1, map A). The most relevant tributary is the Vichtbach. At the most downstream gauging station (20 km upstream of the river's mouth), the Inde has a mean discharge of 2.77 m^3/s, and the mean discharge during yearly reoccurring flood events is 46.57 m^3/s [90]. All-year precipitation has a slight maximum in the summer months when intense precipitation events can lead to flood events with steep flood waves, as in summer 2021 (see next section). However, flood events in the winter months are more common due to snow melting in the Eifel mountains [91]. From Stolberg downstream, the Inde and Vichtbach have fully anthropogenically constructed bank structures. They were built in the 1970s as an extensive flooding protection. Ever since then, even the discharge of an event with a reoccurrence interval of 100 years induces only locally limited overflowing of the floodplains.

On its relatively short course of 54 km, the Inde crosses the border from the mid-mountain ridge to the lower Rhine embayment. This results in strongly differing conditions regarding valley shape (from v-shaped to very flat and wide valleys), gradient of the river (from steep to relatively flat), and underlying geology: in the Eifel mountains, the Inde crosses Cambrian to Devonian sedimentary lithologies that are widely covered by periglacial cover beds, and Carboniferous limestones with economically relevant ore deposits. In the lowlands, the catchment is underlain by Quaternary sediments (mainly loess) (Fig. 1, map B). The Vichtbach, on the contrary, entirely flows in the mountainous area. It is very steep, with quick-flowing flood waves. In the upper reaches, there are, in many places, no extended floodplains. Instead, the valleys are v-shaped, and the steep slopes do not allow for the development of sedimentary floodplains.

The Inde catchment was intensely shaped by the mining of hard coal, iron, lead, and zinc ores [92–94]. In addition to the ores, the region was rich in wood for charcoal production and creeks suitable for hydropower usage. This availability of resources led to the establishment of various industries along the streams of the catchment. From the 16th to the beginning of the 20th century, the city of Stolberg, located at the confluence of the Vichtbach and the Inde, became a supra-regional center of the brass and, later on, the glass industry [94, 95]. Many of these industries influenced the river by discharging wastewater directly into the river. In addition, the landfilling of waste material on the company's private land, which was little regulated then, has resulted in an almost unmanageable number of brownfield sites, many located in the floodplain. Furthermore, atmospheric emission of metal-bearing dust induced a widespread enrichment of, among others, Pb and Cd [96]. Detailed information on the Inde catchment and its industrial legacy can be found in Esser et al. [93] and references therein. Today, only a few large-scale industrial units are left. Many of them are located along the Vichtbach in Stolberg, forming a cluster of metalworking industries.

The July 2021 flooding

From July 14th to July 15th, 2021, the Inde catchment was affected by intense rainfall, leading to an extreme flood event. An estimated doubled monthly average of precipitation fell within these two days over large areas of the German-Belgian Eifel-Ardennes, causing severe flooding in most rivers draining the low mountain range (Fig. 2) [97–99]. Many stations recorded their all-time maximum of precipitation within 24 h [100], and overall maxima reached > 150 mm within one day [101]. As this excessive rain, with locally occurring torrential rain, fell on short, steep valleys, it induced a flooding crisis affecting parts of western Germany, Belgium, Luxemburg, France, and the Netherlands [102]. Waterlogged soils aggravated the situation: prior to the days with extreme precipitation, prolonged rainfall of lower intensity caused almost completely water-saturated sediments, thereby inducing quickly flowing surface runoff [101, 103, 104]. This surface flow led to a rapid rise of water levels in the receiving rivers and exceptionally intense erosion along channels and on surfaces [105]. The event is a textbook case of a flash flood with quickly rising water levels, extremely short response times, high flow velocities and transport capacities, and consequential intense erosion [106]. Extensive descriptions of the event can be found in Dietze et al. [104], Mohr et al. [102], Ludwig et al. [107], and Lehmkuhl et al. [98].

In the immediate aftermath of the flooding, when the extensive deposition of flood sediments became apparent, concerns arose due to the possible contamination of the sediments [108]. The exceptionally high water levels caused overflowing in areas usually unaffected by flooding, which activated additional pollution sources, as

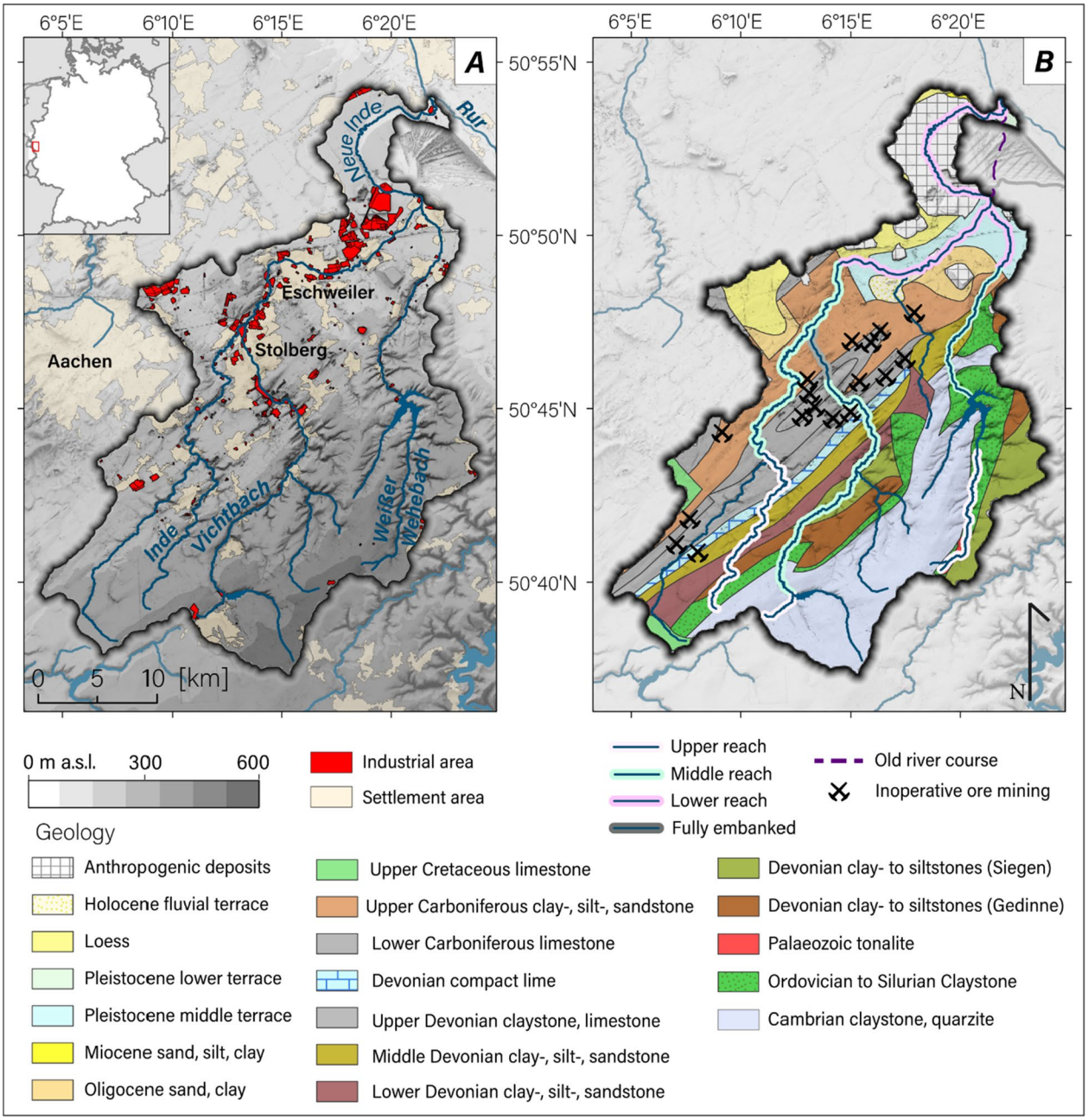

Fig. 1 General map (**A**) of the Inde River catchment with its main tributaries, Vichtbach and Wehebach, and a geologic map (**B**) of the catchment. The most downstream part of the Inde was relocated in 2007 due to the progression of an open-pit lignite mine. The relocated reach is named "Neue Inde" (translates to "New Inde"). The settlement and industrial center is around the towns of Stolberg and Eschweiler, where the center of the ore mining and processing industries was located

shown by enhanced pollutant levels in the exceptionally widespread deposited sediments [109, 110].

Sampling

In the aftermath of six different high-discharge events (April 2018, June 2018, January 2019, March 2019, July 2021, and February 2022), freshly deposited fluvial sediments were collected. All sampling points are depicted in Fig. 3. The fine-grained material was scratched from vegetated or, if the flooding extent reached settlement areas, sealed surfaces like pavements or asphalt and stored in Whirl Pacs until further analysis. Details on the six

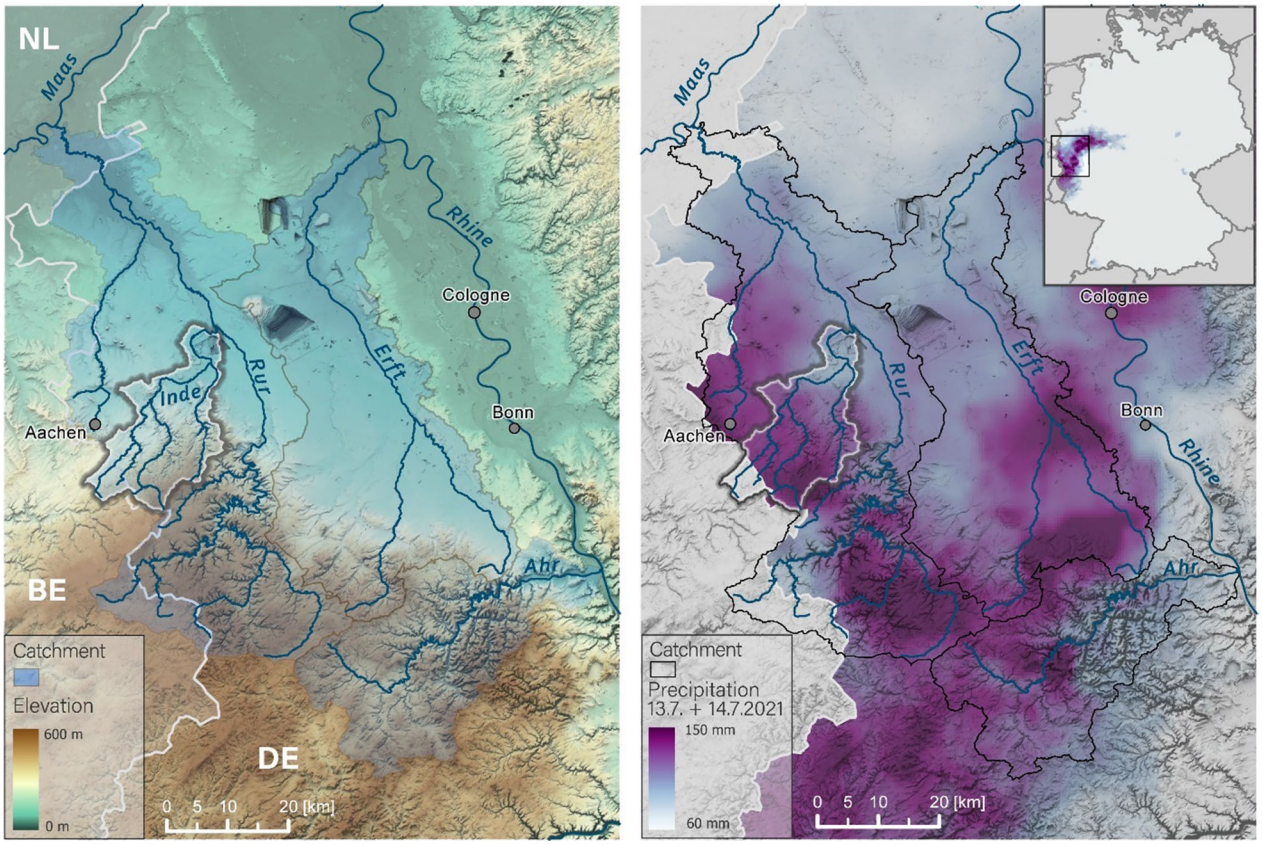

Fig. 2 The catchments most affected by the July 2021 flood event. Rainfall data is based on REGNIE hourly precipitation data, which is only available for Germany. The highest rainfall intensities (right map) coincide with areas with upstream midrange mountain areas with short, steep valleys (left map). This combination led to an unexpectedly quick rise in water levels, resulting in a devastating flash flood

events and the sampling locations are given in the supplement. Four of the six events were < HQ_5 (HQ_5 describes an event with a reoccurrence probability once every 5 years), which entails bankfull discharge and, occasionally, minor flooding of the proximal floodplain. In March 2019, the HQ_5 threshold was exceeded at some gauging stations. By far, the most intense event was the flood in July 2021, which has already been described in detail. The extremely high water levels led to the widespread deposition of fine flood sediments [110].

In addition, in March 2022 and July 2023, bank material was sampled to provide further insight into the trend of trace element enrichment in the fluvial sediments in the aftermath of the extreme event in July 2021. Bank sediments are of particular relevance for trace element assessment because of the rapid cycling of these sediments and the exposure to bioturbation, water movement in the hyporheic zone, and changes in redox state, all contributing to a potential increase of the bioavailability of possible risk elements [111, 112]. The specific geomorphologic situations were considered, and we carefully selected sampling spots where deposition of sediments at slightly elevated discharge is expected. This sediment can be seen as part of the throughput load and is a recommended endpoint for assessing river pollution [113]. Samples were collected by using a spade to extract cubes with an edge length of 20 cm. These cubes were sampled evenly along the 20 cm depth. If the lower limit of the sediments of the July 2021 flood was clearly recognizable, the sampling was limited to these sediments. However, this was the exception, probably because, in most sampling locations, more sediment was deposited during the 2021 extreme flood.

Furthermore, to gain insight into the anthropogenic enrichment of trace elements with respect to their geogenic background, we sampled topsoils in the floodplains of the upper Inde catchment in places where anthropogenic influence is minimal (see Figs. 1 and 3). The sampling was limited to siliclastic lithologies, even though smaller parts of the catchment are underlain by calcareous bedrock. As the area of outcropping carbonates is small and intensely anthropogenically influenced, it is unsuitable for any baseline sampling. Eighteen samples were collected along the upper Inde River itself. Here,

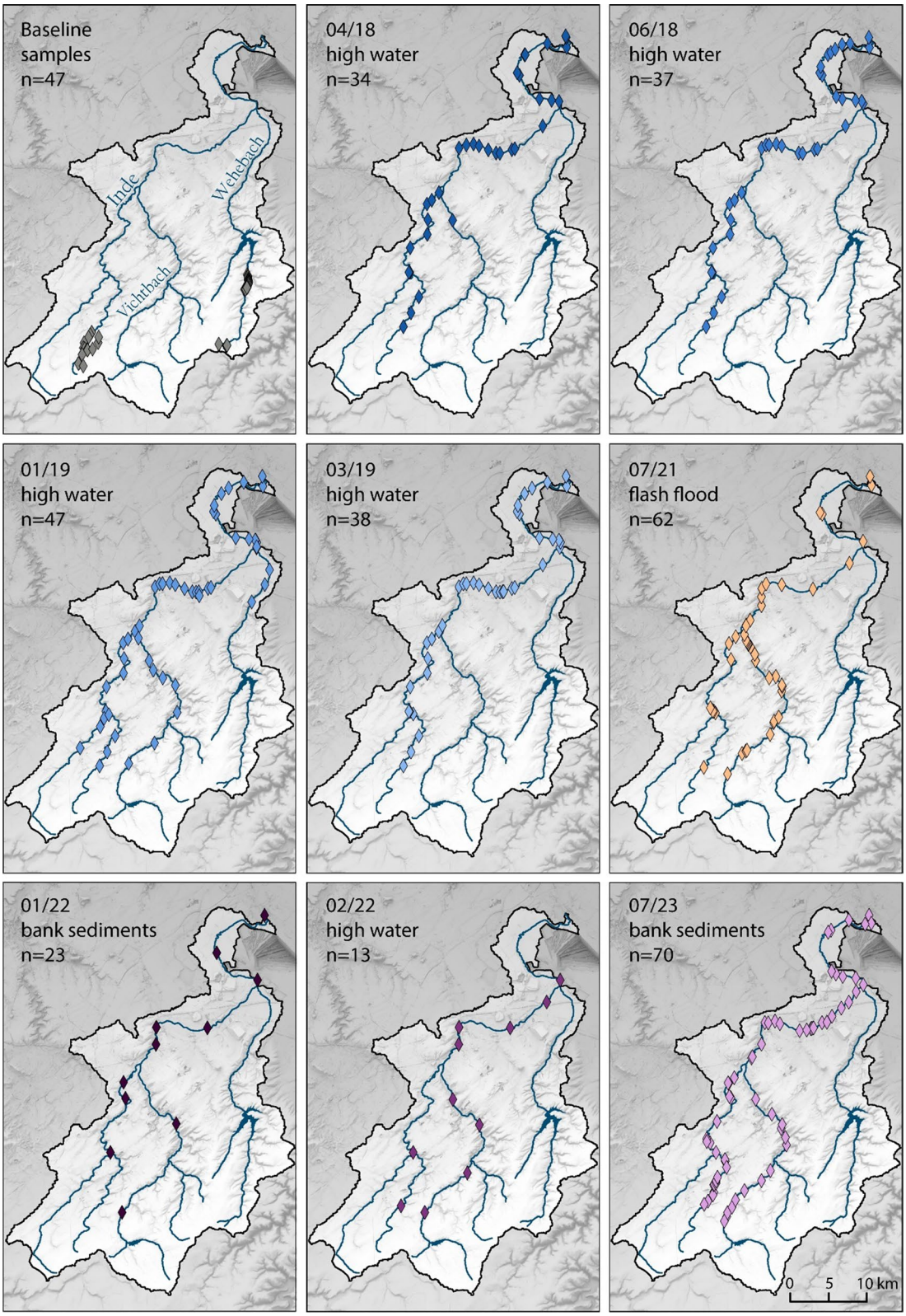

Fig. 3 Overview map of the nine sampling campaigns conducted in the Inde catchment from 2018 to 2023. In addition, the number of samples and the objective of each campaign are given. The color scheme will be applied in all further figures differentiating the sample sets

the Inde flows in a fairly natural environment within an inhabited protected landscape with sporadic forestry use. The "Weißer Wehebach", a tributary of the Wehebach, which flows into the Inde (see Fig. 1), is classified as the river with the most natural condition within the Inde River Basin. Therefore, another set of topsoil samples was collected in its floodplains. The sampling technique was identical to the bank samplings.

Laboratory analysis

Samples were dried at 35 °C and larger organic particles were removed by hand before being carefully ground using an agate mortar and sieved to < 2 mm. For the analysis of elemental concentrations, the remainder of the samples was fully dried at 105 °C for 12 h. 8 g of the sediment were mixed with 2 g Fluxana Cereox binder, homogenized by shaking, and pressed to a pellet by applying a pressure of 19.2 MPa for 120 s. Energy-dispersive polarized X-Ray fluorescence (XRF) (Spectro Xepos) measured elemental compositions in duplicate with rotation of the pellet in between measurements, and the arithmetic means were used for further analysis [114], which focused on Ti, V, Cr, Co, Ni, Cu, Zn, Ga, As, Rb, Sr, Y, Zr, Nb, Cd, Sn, Sb, Ba, Nd, Hf, Pb, and Th. Measurements were calibrated using certified reference materials of soils (CRM No. 5360-90, CRM No. 5358-90, CRM No. 2499-83, CRM 2505-83, CRM 2508-83, CRM No. 5359-90, SARM 42, USGS GXR-2, GXR-5, and GXR-6). All XRF measurement results, their root mean errors, and the element's detection limits are provided in an Excel spreadsheet as part of the supplementary material.

To assess grain size distribution, the organic material was removed by treating the sediment repeatedly with 0.70 mL 30% H_2O_2 at 70 °C for several hours until the material bleached. Samples were also treated with 1.25 mL $Na_4P_2O_7$ (0.1 mol*L^{-1}) overnight with an overhead shaker to ensure the dispersion of particles [115, 116]. Laser diffraction measurements were performed using a Beckman Coulter LS 13 320. The resulting 116 particle size classes indicate the percent size frequency of particles from 0.04 to 2000 µm with an error of 2%. Particle size distribution was calculated using the Mie theory (Fluid RI: 1.33; Sample RI: 1.55; Imaginary RI: 0.1) [117–119].

Calculation of a local geochemical baseline and a local enrichment factor

Among the many factors determining the trace element concentrations in sediments are the geologic source region, the content of organic material and Fe–Mn oxides, and sediment sorting [49, 120–123]. Therefore, any assessment of enrichment of trace elements needs to be done based on a reference level to investigate deviations from these expected concentrations. Only such a baseline allows for distinguishing anthropogenic influences from natural concentrations. However, as a precise definition of this level on a local scale is often unavailable, many authors rely on global means, such as the elemental composition of the upper continental crust. While this might be suitable for large-scale studies, it is only of limited use for locally limited sampling sets. Even more so if the sampling area is dominated by anomalies, such as the occurrence of specific ores. Moreover, a background concentration must be based on maximum homogeneity [124]. Hence, it should be calculated for a specific environmental compartment [123]. Therefore, mean concentrations calculated for rock material are not ideal for evaluating weathered fluvial sediments.

Matschullat et al. [124] define the background as the naturally occurring concentration range of any trace element in anthropogenically non-influenced samples. However, as the Inde catchment is densely populated, a ubiquitous anthropogenic influence has to be assumed (e.g., by atmospheric deposition), which cannot be excluded by any sampling strategy. Therefore, we use the term *baseline* and define this as the upper limit of the naturally occurring concentration plus the ubiquitous anthropogenically induced enhancement of trace elements, following the definition by Salminen & Gregorauskien [125].

Baseline levels were calculated using the iterative 2σ-approach (described in great detail in [124]), a method suitable for right-skewed distributions [124]. It was shown to provide meaningful results specifically for the Inde catchment [91]. A sometimes criticized drawback of this approach is its limited applicability if a larger number of outliers is included in the dataset [47, 126]. However, as the 47 samples used as input for the calculation were collected in the less anthropogenically impacted upper catchment (Fig. 3) from comparable sediment types, no strong influence of actual outliers is expected. Moreover, relying on the mean + 2σ-method provides a high upper threshold of naturally occurring concentrations [126]. This, in turn, results in more conservative estimates of the anthropogenic influence.

One of the widely acknowledged difficulties in assessing flood sediment chemistry is the grain size dependence of many trace elements that are preferably found in finer sediments [14, 46, 127]. Hence, the grain size sorting inherent in flood sediments inevitably influences the trace element concentration [17], making correcting for textural biases imperative to compare different locations and events.

To this end, a local enrichment factor (EF) based on the baseline sample set [128] was calculated as

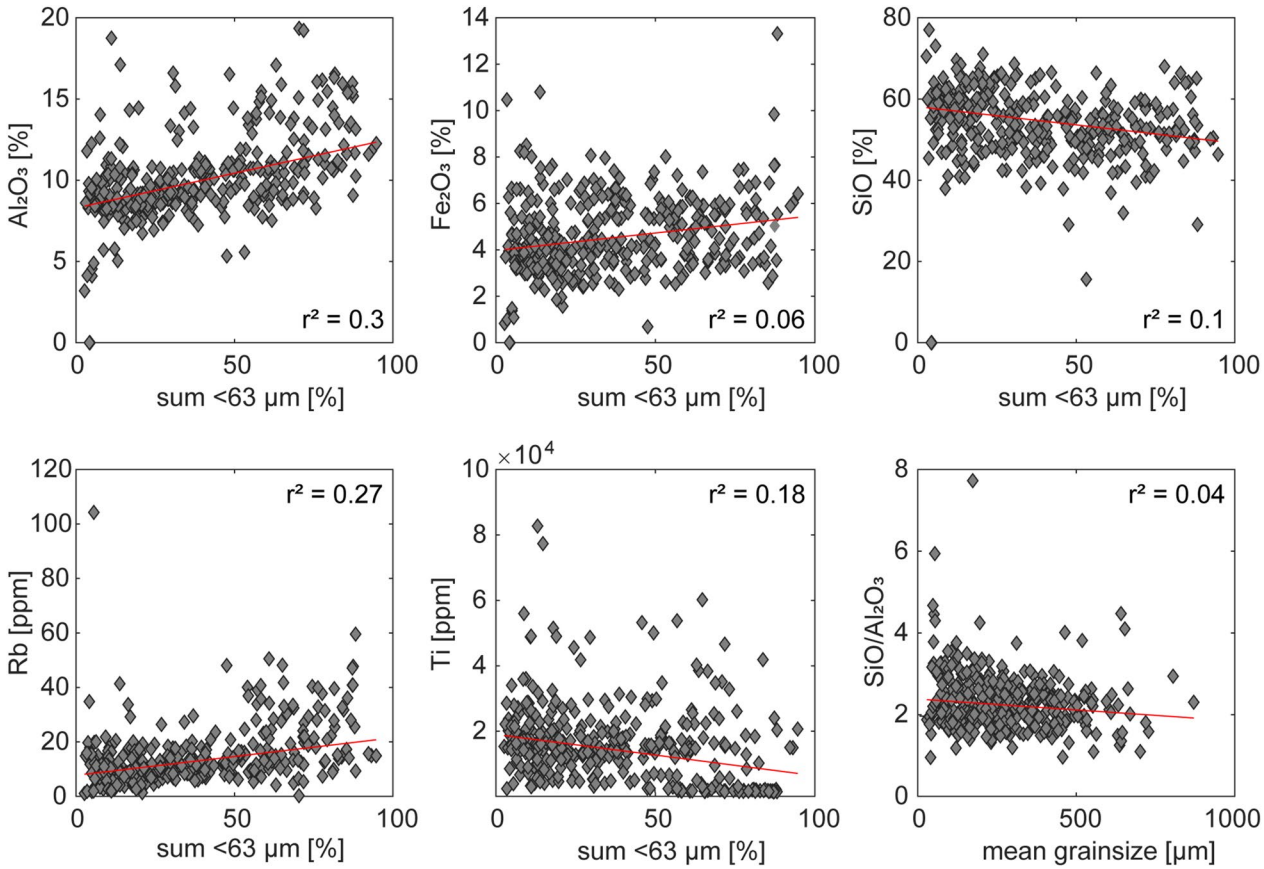

Fig. 4 The six plots depict the relation of the grain size, either given as sum of all grain size classes < 63 µm or as mean grain size, and common geochemical parameters used to approximate grain size characteristics. In addition, the coefficient of determination r^2 is given. For Al_2O_3, Fe_2O_3, Rb, and Ti, higher concentrations are expected in finer sediments, whereas the SiO content and the ratio of SiO to Al_2O_3, should decrease in finer sediments. Based on r^2, the Al_2O_3 content is the most suitable approximation of the fine material. Hence, Al was chosen as reference element for geochemical normalization

$$EF = \frac{c(TE_{sample})/c(Ref_{sample})}{c(TE_{baseline})/c(Ref_{baseline})} \quad (1)$$

where c(TE) is the concentration of the trace element investigated in a specific sample or the calculated baseline, respectively, and c(Ref) denotes the concentration of a reference element. This reference element, which should function as an indicator for the above-mentioned natural variations in concentrations, needs to be grain size sensitive, free of anthropogenic impact, and conservative within sediments, i.e., not prone to translocation processes [46, 47].

As Matys Grygar [129] pointed out, the usefulness of any selected reference element to predict the element of interest's behavior has to be thoroughly checked. Some widely used grain size indicators were plotted against grain size parameters, and a robust regression was calculated to test their grain size dependence (Fig. 4 and Fig. S5 in the supplement). Of the six proxies tested, only Al provided acceptable results with a $r^2 = 0.3$. Hence, as a next step, we checked the covariance of Al and the defined elements of interest in the baseline samples (Fig. 5). We found acceptable correlations for some elements (like Ti, V, Cr, Cu, Zn, Ga, Rb, Sr, Y, Nb, Ba, Nd, and Th). However, for other elements, no correlation with Al was found. This applies mainly to elements known to be anthropogenically influenced, like Ni, As, Cd, Sn, Sb, and Pb, but also Zr and Hf. Regarding the former, atmospheric deposition might play a role: atmospheric input of trace metals was documented even for remote areas of Germany [130] and was a major problem for the area of Stolberg in the 1980s due to the intense industrial activities [96]. Therefore, even though the calculation of baseline concentrations based on regressions, as described in detail by Matys Grygar and Popelka [47], is recommended, we opted to calculate an upper threshold as the baseline. This baseline includes ubiquitous enrichment

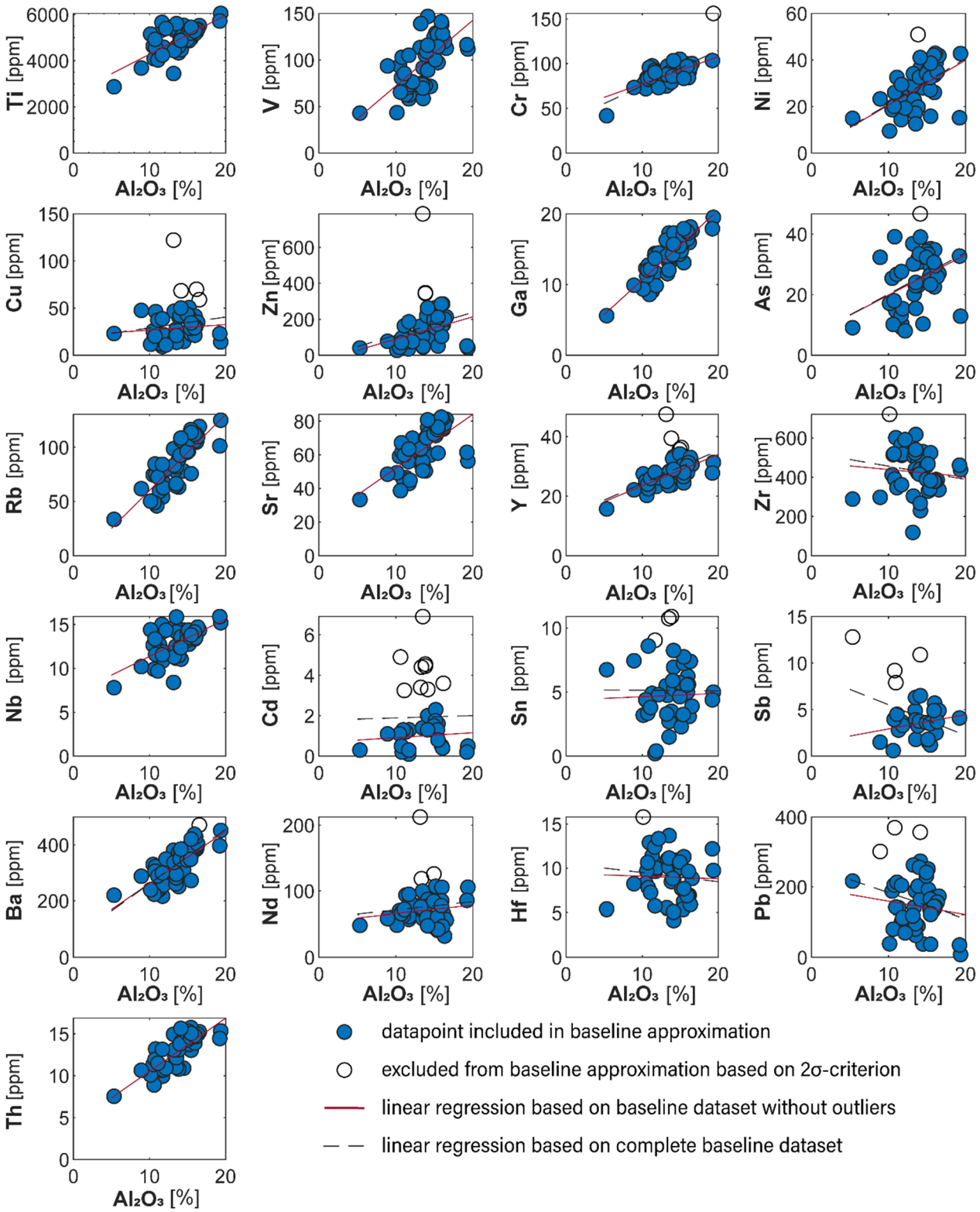

Fig. 5 Correlation of the Al concentration (x-axes) and the concentration of the investigated trace elements (y-axes) in the baseline samples. Empty circles indicate samples excluded from the baseline assessment based on the 2σ-iteration. Elements known for some level of ubiquitous anthropogenic influence (such as Pb, As, or Sn) exhibit some scatter. However, elements with limited anthropogenic impact (like Cr, Ga, Ba, or Th) do not deviate markedly from an interrelation with Al. Therefore, we conclude that Al is a suitable element to cover the natural variability of trace elements

due to atmospheric deposition and, again, provides rather conservative estimates of the anthropogenic input into the sedimentary system due to fluvial processes. Despite the minor correlations with possibly anthropogenically influenced trace elements, Al was chosen as a conservative reference element because of its clear correlation with elements like Rb or Th, which are usually not anthropogenically influenced, and its ability to serve as a grain size proxy.

Testing for differences in sample sets

The Shapiro-Wilks test was used to test for a standard normal distribution [131] of all subsample sets (i.e., for the 8 events and 22 elements, resulting in 176 subsets). As the majority of the sets were not normally distributed, non-parametric statistics were used to compare the datasets. Using the Kruskal–Wallis test (KW-test), the 8 subsets of each element's enrichment were compared to each other to gather information on the difference between datasets and, hence, the influence of the flash flood on trace element enrichment in the fluvial sediments.

Positive matrix factorization

The basic idea of FA is a bilinear model:

$$X = GF + E \tag{2}$$

with X being a matrix of observations with m samples and n measured properties for each sample [132]. This matrix can be factorized into two smaller matrices, *G* and *F*, often labeled as scores and loadings. *E* denotes the error, i.e., the variation in the input data not covered by the product of *G* and *F*. Based on this equation, the residual matrix can be denoted as

$$E_{ij} = X_{ij} - \sum_{h=1}^{p} G_{ih}F_{hj};\ i = 1,\ldots,m;\ j = 1,\ldots,n;\ X = m \times n;\ G = m \times p;\ F = p \times n \tag{3}$$

where p symbolizes the selected rank of the model, i.e., the number of modeled factors.

PMF, as introduced by Paatero and Tapper [66], aims to solve the factor analytical problem by applying a weighted least squares approach. Under the constraint of non-negativity, the object function Q (Eq. 4) is iteratively minimized.

$$Q(E) = \sum_{i=1}^{m}\sum_{j=1}^{n}\left(\frac{E_{ij}}{\sigma_{ij}}\right)^2 \tag{4}$$

Here, the residuals E are weighted with the data point-specific error estimation σ, called uncertainty [88]. The resulting Q is often referred to as Q_{true} [58]. This approach makes ideal use of data characteristics in physical sciences, where experimental uncertainties are usually available, and accuracies within columns and rows are unsteady [133]. Thus, potential outliers and the typical right-skewed distributions, which are an integral part of environmental analysis [66], can be included in the modeling process [134]. Furthermore, missing data and data below the detection limit can effectively be included in the analysis by enhancing the uncertainty of respective data points [70, 82].

PMF can be applied in robust mode to further limit the influence of extreme values. The resulting Q_{robust} is defined as:

$$Q_{robust}(E) = \sum_{i=1}^{m}\sum_{j=1}^{n}\left(\frac{E_{ij}}{h_{ij}\sigma_{ij}}\right)^2 \tag{5}$$

$$h_{ij} = \begin{cases} 1 & for\left|\frac{E_{ij}}{\sigma_{ij}}\right| \le \alpha \\ \left|\frac{E_{ij}}{\sigma_{ij}}\right| \Big/ \alpha & for\left|\frac{E_{ij}}{\sigma_{ij}}\right| > \alpha \end{cases} \tag{6}$$

which limits the outlier distance incorporated into the minimization process to α [58]. A commonly applied value is $\alpha = 4$.

The uncertainty calculation is a crucial step in PMF modeling [66]. The approach, including the handling of missing values and concentrations below the detection limit, as established by Pollissar et al. [70], is used in the majority of PMF publications [58]. It takes into account the detection limit and the analytical uncertainty. However, there is no linear relationship between analytical error and measured concentration for most compounds analyzed in this study. Moreover, their distributions are mostly right-skewed. Therefore, introducing an additional parameter accounting for the concentration value itself was necessary. By doing so, the uncertainty of high-concentration values is dominated by their concentration, so possible outliers are downscaled. On the other hand, the uncertainty of small-concentration data points is dominated by the detection limit and measurement uncertainty [135]. Hence, for uncertainty calculation, a combination of the approaches by Polissar [70] and Vaccaro [82] was applied:

$$\sigma_{ij} = \begin{cases} \sqrt{u_{ij}^2 + \left(\frac{dl_j}{3}\right)^2 + \left(d_j x_{ij}\right)^2}, & for\ x_{ij} > dl_j \\ 5/6\, dl_j, & for\ x_{ij} \le dl_j \end{cases} \tag{7}$$

Table 1 Parameters indicating the model's quality for solutions from 2 to 8 factors. Even though some parameters improve by adding more factors (because the model covers a larger part of the data's variance), the impairment of indicators like DISP and bootstrapping reveals that this is actually overfitting. Furthermore, the various Q-ratios point to only minor improvements for more than five factors. Hence, five factors are deemed ideal

Number of factors	2	3	4	5	6	7	8
$Q_{expected}$	6252	5863	5474	5085	4696	4307	3918
Q_{true}	28,513.1	16,454.2	10,834.6	6389.7	4626.8	3684.7	2919.8
Q_{robust}	20,672.5	13,726.2	9307.1	6195.3	4539.6	3619.8	2861
Q_{true}/Q_{robust}	1.38	1.20	1.16	1.03	1.02	1.02	1.02
$Q_{robust}/Q_{expected}$	3.30	2.34	1.70	1.22	0.97	0.84	0.73
$Q_{true}/Q_{expected}$	4.56	2.81	1.98	1.26	0.99	0.86	0.75
Species with $Q/Q_{expected} > 6$	4	2	1	0	0	0	0
DISP %dQ	−0.472	0	0	0	−0.019	0	−0.195
DISP swaps at $dQ_{max} = 4$	0	0	0	0	0	0	0
N° of factors with mismatched bootstrap runs (and their respective percentage)	0	1 (28%)	3 (5%, 7%, 13%)	1 (1%)	2 (1%, 2%)	2 (8%, 2%)	4 (9%, 14%, 2%, 8%)
BS-DISP % cases with swaps	–	–	–	0	–	–	–

with u_{ij} being the analytical uncertainty of the j^{th} element in the i^{th} measurement, dl_j the detection limit of the j^{th} element, and x_{ij} representing the measured concentration of the j^{th} element in the i^{th} sample. The element-specific factor d_j is a proportional coefficient, as proposed by Vaccaro et al. [82] for the PMF analysis of XRF-measured concentrations of trace elements. For elements not covered by their approach, $d_j = 0.15$ was assumed. For Cd, Sn, and Sb that have low abundance, d_j was set to 0.25. Even though this is somewhat arbitrary, it seems reasonable as it is within the range of the established d_j values, and Vaccaro et al. [82] showed that changing the coefficients by a factor of 2 does not significantly influence the resulting factor structure. Details are provided in Table. S3.

Included elements were limited to trace metal(oid)s with a signal-to-noise ratio (S/N) of $S/N > 2$ (calculated following [89]). Exceptions were made for Cd ($S/N = 1$) and Sb ($S/N = 0.9$) because they are relevant pollutants in the Inde catchment [110, 136]. To account for their low S/N, their uncertainty was tripled [89]. In addition, Co was excluded because it induced difficulties in the modeling process (i.e., by quickly generating a factor purely dominated by this element). In summary, the following elements were included in the PMF model: Ti, V, Cr, Ni, Cu, Zn, Ga, As, Rb, Sr, Y, Zr, Nb, Cd, Sn, Sb, Ba, Nd, Hf, Pb, and Th. For details on the settings, see Table S2. PMF calculation was done using EPA PMF 5.0.

One of the critical steps in modeling using PMF is deciding on the number of factors that offer an ideal representation of the observed data without overfitting the model to the data's inherent noise [64]. Solutions with 2 to 8 factors were tested. Table 1 displays a detailed comparison of the respective results. For details on the parameters mentioned in the following passage, the reader is referred to publications focusing on the methodological aspects of PMF [58, 67, 89, 137–139].

For a start, the investigation of the Q values is helpful. A ratio of $Q_{true}/Q_{robust} = 1$ would imply a model not influenced by any outliers. However, this might only be reached when the model is overfitted. Up to five factors, the ratio shows a significant decrease for each factor added, whereas adding a sixth factor leads to only minor improvements in the ratio (Table 1). Moreover, the five-factor solution is the first one with all species below the threshold of $Q/Q_{expected} < 6$, that Brown et al. [137] suggested. Q_{true} and Q_{robust} values were stable for the 100 model runs conducted. For an ideal model, the object function Q approximates the degrees of freedom, defined as

$$Q_{expected} = mn - p(m + n) \tag{8}$$

with p denoting the number of factors and m and n defining the size of the input matrix, but only accounting for non-weak entries [89, 139]. $Q/Q_{expected} < 1$ implies overfitting; hence, five factors are the largest amount of factors possible with overfitting (see Table 1).

Bootstrapping-displacement (BS-DISP) is computationally expensive, especially for large datasets [137], so it was conducted only to check the final solution. The selected five-factor solution provided excellent results: no drops of Q, no swaps in best fit, no swaps in the DISP phase, and no factor swaps for any dQ_{max} levels. The results of BS-DISP are deemed especially meaningful since they include the effects of random errors as well as rotational ambiguity [89, 137]. As rotations using the

F-Peak tool did not clearly improve the model, based on inspection of changes in G-space plots [138, 140], no rotation was applied to the final model.

The selected five-factor model is generally of high quality and performed best in the bootstrapping (BS) and displacement (DISP) analysis among the tested solutions (Table 1). Four of the five factors were remodeled in 100% of the 100 BS runs. The only mismatched run was found for the Cu-dominated factor, which, in many samples, has no contribution. The DISP analysis resulted in no drops of Q and no factor swaps. Adding a sixth factor leads to splitting the factor dominated by Cu and Sn into two factors (Fig. S6 in the supplement), each representing mainly the variance of each species. However, they exhibit strong co-occurrence (with a correlation of $r = 0.6$, $p < 0.001$). Therefore, modeling them into one factor seems reasonable.

Looking into element-specific errors, some compounds have higher errors (Fig. 6). However, for all elements used for factor identification (factor 1: Zr, Hf; factor 2: Cu, factor 3: Sb, Pb; factor 4: V, Rb; factor 5: Zn, Cd, Pb, As, for details see results chapter), only minor errors were found in BS, DISP, and BS-DISP analysis in the respective factors. In addition, they all have a reasonably high coefficient of determination ($r^2 > 0.7$) between observed and predicted concentrations (see Tab. S3 in the supplement) except for Hf ($r^2 = 0.49$) and Sb ($r^2 = 0.69$). Cr, Sr, Ba, and Nd have lower r^2 (0.4), but no factor's identification relies on these elements.

Results

Comparison of the geochemical signatures of the flood sediments

For the four flood events from 2018 to 2019 (all $\leq HQ_5$), a very uniform pattern was found: the four events exhibit similar geochemical fingerprints with only a few exceptions, that are limited to elements with a generally low EF (Nd 04/18-03/19; Sn 04/18-01/19; Rb 04/18-01/19, 04/18-03/19; Sr 04/18-01/19, 04/18-03/19, 06/18-01/19, 06/18-03/19; Ba 04/18-01/19; 04/18-03/19, 06/18-01/19). All results from the subset analysis are depicted in Fig. 7.

When looking at all datasets (including the extreme events and the samples taken during the following years), no uniform trend can be identified for all trace elements. Instead, there are groups of elements for which a typical behavior can be determined. A clear differentiation between elements indicating supply through human activities and rather natural elements is evident, which were merged into Groups A and B, respectively. Based on the differences in enrichment between different events, the two groups were further divided into subgroups (A.1, A.2, A.3, B.1, and B.2).

Pb, Cd, Cu, As, and Zn form **Group A.1**. The flash flood led to a marked increase in enrichment for these elements. In the aftermath of the extreme event, there is a decrease in enrichment with different rates of change between the elements. According to the KW-tests, two years after the flash flood, the enrichment factors of these elements are comparable to the situation before the extreme event. However, the boxplots exhibit a pronounced upper tail of the distributions, pointing at a general downward trend but with several sampling points still strongly affected by the intense input of these elements during the flash flood. The influence of the topmost quartile of enrichment values is apparent for Zn: the KW-tests reveal almost no differences between events. However, inspection of the boxplots shows much higher enrichments since the extreme event, even though they seem locally limited. **Group A.2** is characterized by a substantial increase of EF only during the extreme event. All events before and after exhibit the identical distribution of low EF. This singular peak implies the influence of a source that only gets activated during extreme events. This group solely comprises Sb. The elements in **Group A.3**, namely Sn and Ni, have similar enrichments for all events according to the KW-tests, implying no influence of the extreme event. Nevertheless, in some samples, the EF is $>>1$, indicating that these elements are exceeding the baseline, hinting at an anthropogenic source that seems active independently of flood events. Consequently, there is no detectable degradation trend in the years after the flash flood.

Group B.1, consisting of Co, Cr, Zr, Y, Ti, Nd, Nb, Hf, and Th, responds with a downward level shifting to the flash flood. For the four events prior to 2021, the enrichments are on a fairly stable level. However, enrichments dropped markedly from the extreme event onward and are now closer to $EF = 1$. Enrichments stayed consistently at the new low level for Co, Cr, Zr, and Y. For Nb, Hf, and Th, slightly lower enrichments are found for the 2023 sample collective. The elements of **Group B.2**, Rb, Ba, Sr, Ga, and V, have a low enrichment in common, but no clear distinction for before and after the extreme flood event can be identified. A slight downward trend is found for some elements (Sr, Rb, and Ba), whereas other elements (Ga and V) do not show any trends. According to the KW-test, there are some differences between the populations, but as the enrichments fluctuate around 1, these are assumed to represent natural variances. The assumption that these elements are influenced mainly by natural processes is further supported by their small concentration ranges [57, 141] and the low skewness of their EF distributions, as can be seen from the boxplots (Fig. 7).

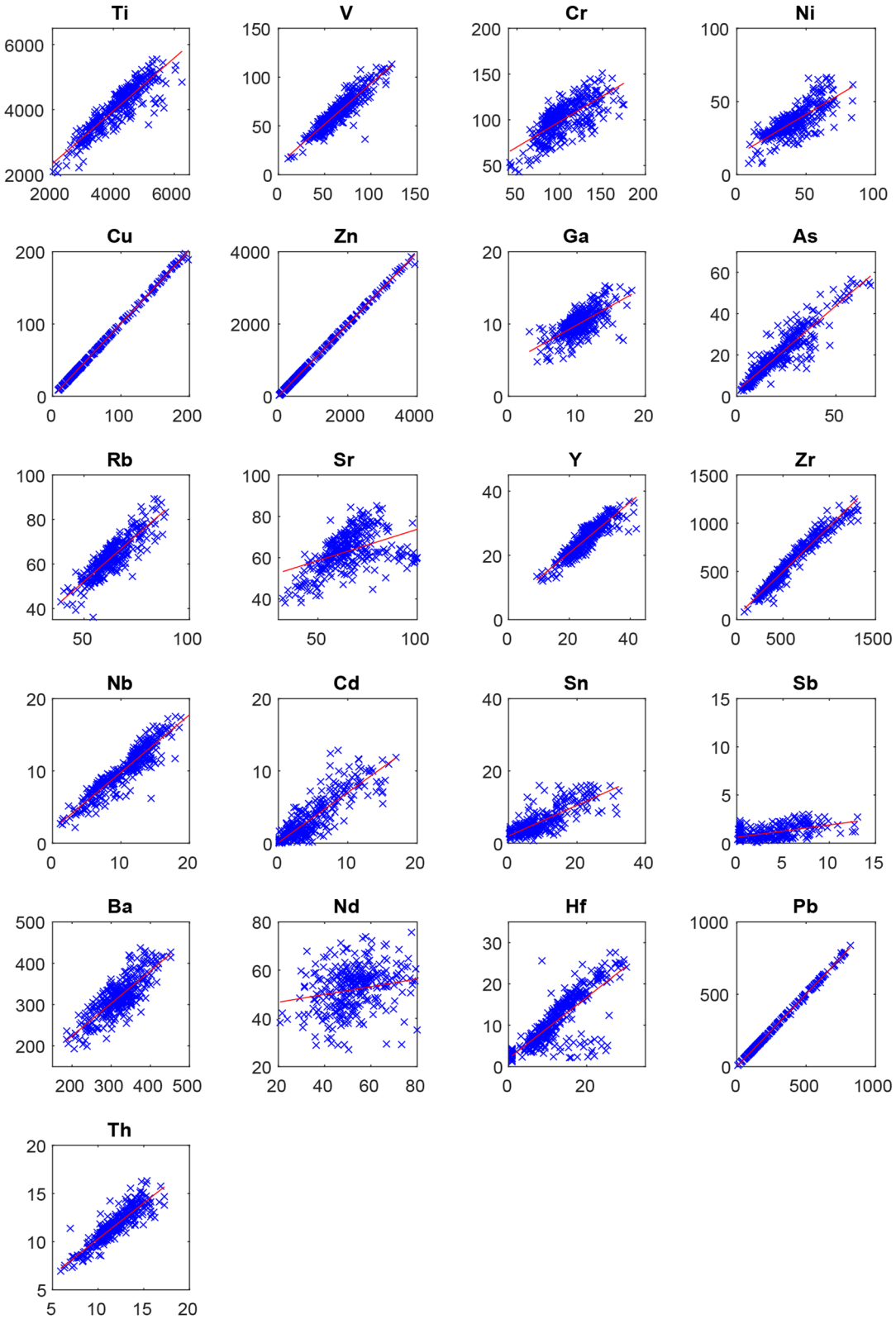

Fig. 6 Scatter plots of concentrations observed on the x-axes vs. predicted by the PMF model on the y-axes. The red line indicates a linear fit. For elements that factor identification is based on, observed and modeled concentrations are in good agreement

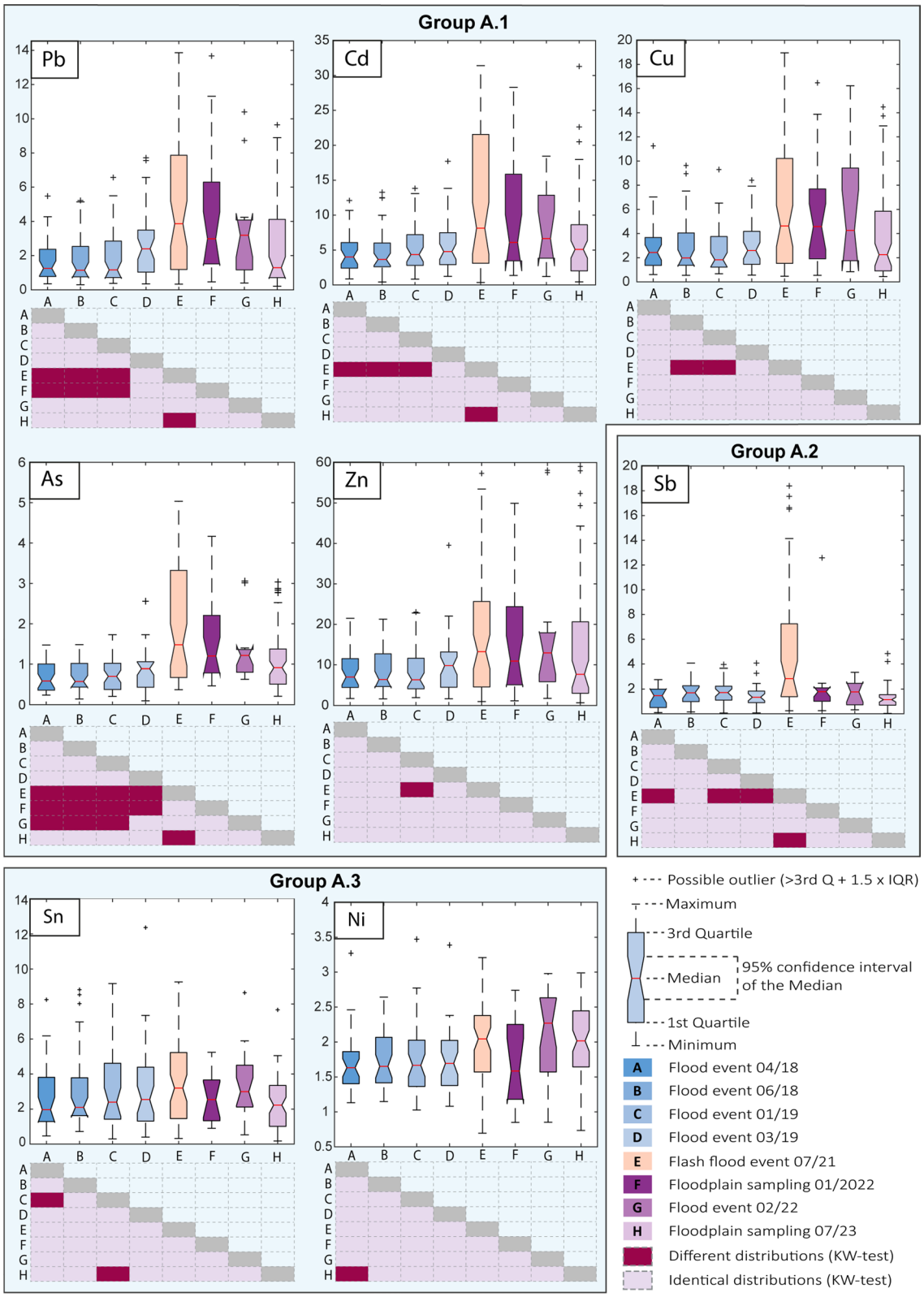

Fig. 7 Notched boxplots of the trace elements' EF (y-axis) for the eight sample sets. For each element, the results of the KW-tests are given in the table below the plot, with darker red indicating a significant difference on the 0.05 significance level and bright red indicating no significant difference between the two populations. The elements are grouped based on concentration trends. For a detailed explanation, see the text. Sequel of Fig. 7. For an explanation of symbology, see Fig. 7, part 1

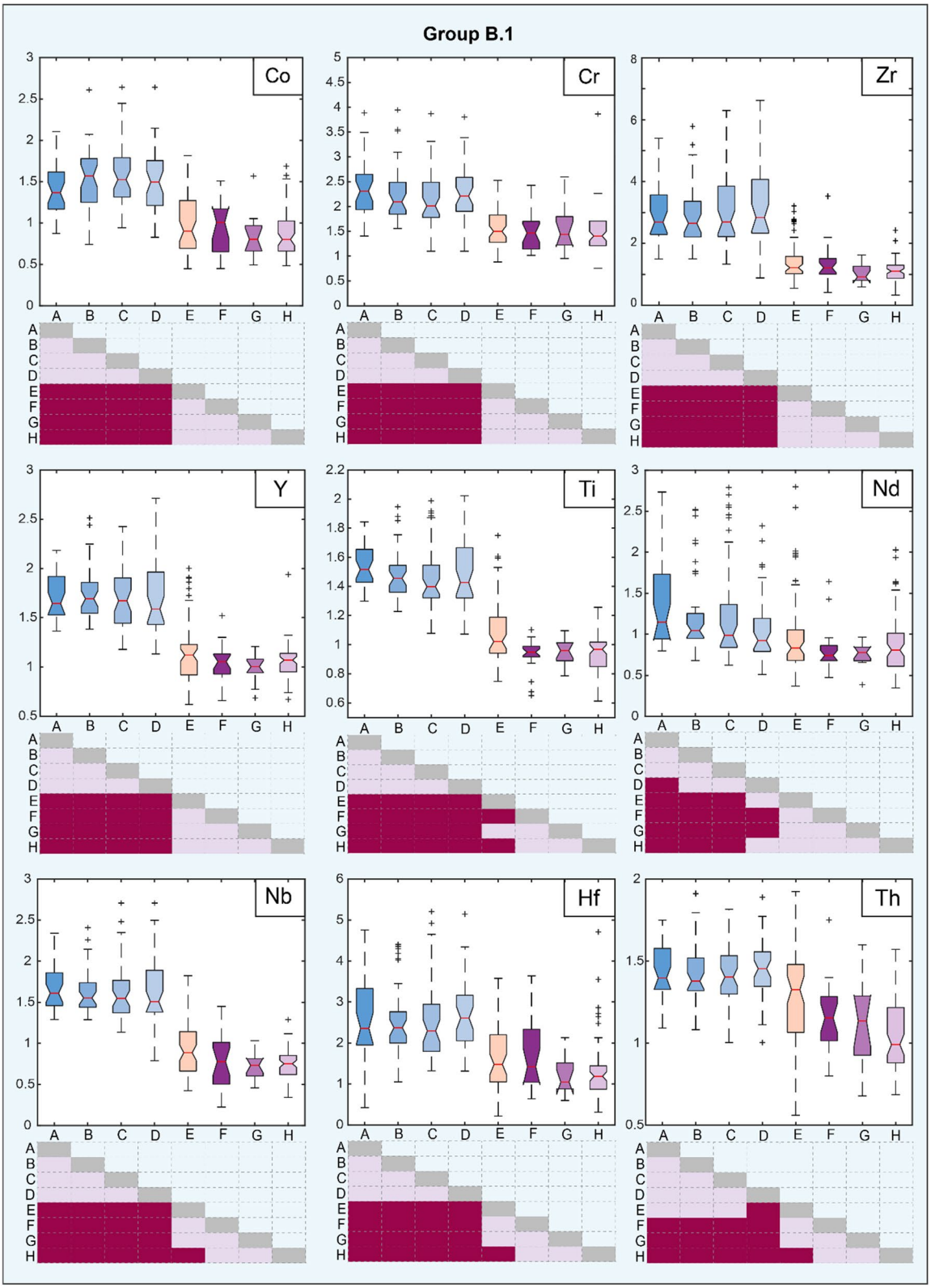

Fig. 7 continued

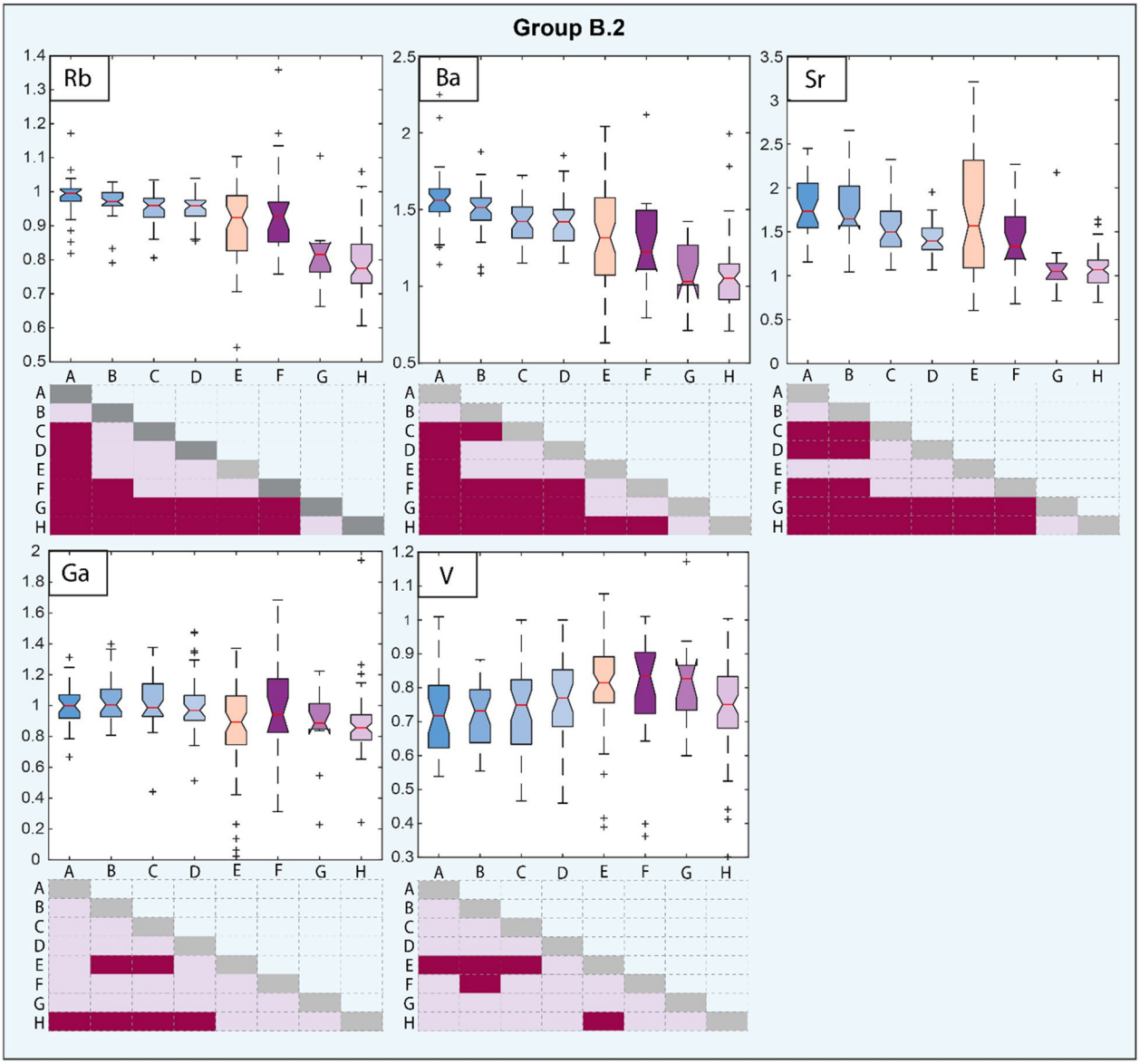

Fig. 7 continued

PMF results

Factor identification

Factors 3 to 5 are dominated by elements primarily associated with anthropogenic emissions [65, 85, 142–144], whereas factors 1 and 2 are dominated by elements occurring rather naturally in sediments (Fig. 8) [85, 142, 145]. This classification is supported by factors 3 to 5 exhibiting a wide range of normalized factor contributions over all samples, while factors 1 and 2 are within a limited range and do not exhibit pronounced fluctuations but relatively steady behavior (Figs. 10, 11), and by the enrichment levels found for these elements (Fig. 7). Factor contributions indicate the contribution of each factor to the total mass by sample. These contributions are normalized to an average of 1 [89].

Factor 1 is dominated by V, Ga, and Rb with 75%, 74%, and 63%, respectively. In addition, Nd, Ba, Ti, Th, Sr, Y, Ni, As, and Nb significantly contribute in the range of 35–50%. Detailed information on the factor profiles is visualized in Fig. 8. The main elements in factor 1 have low enrichment factors of close to 1 (Fig. 7), hinting at naturally occurring sediments as the source for factor 1. V, Ti, Ni, Th, Rb, Y, Nd, and As are often used as markers for naturally occurring sediments [62, 65, 83, 85, 141, 142, 144, 146–151]. Therefore, factor 1 is interpreted to account for a background signal representing sediments

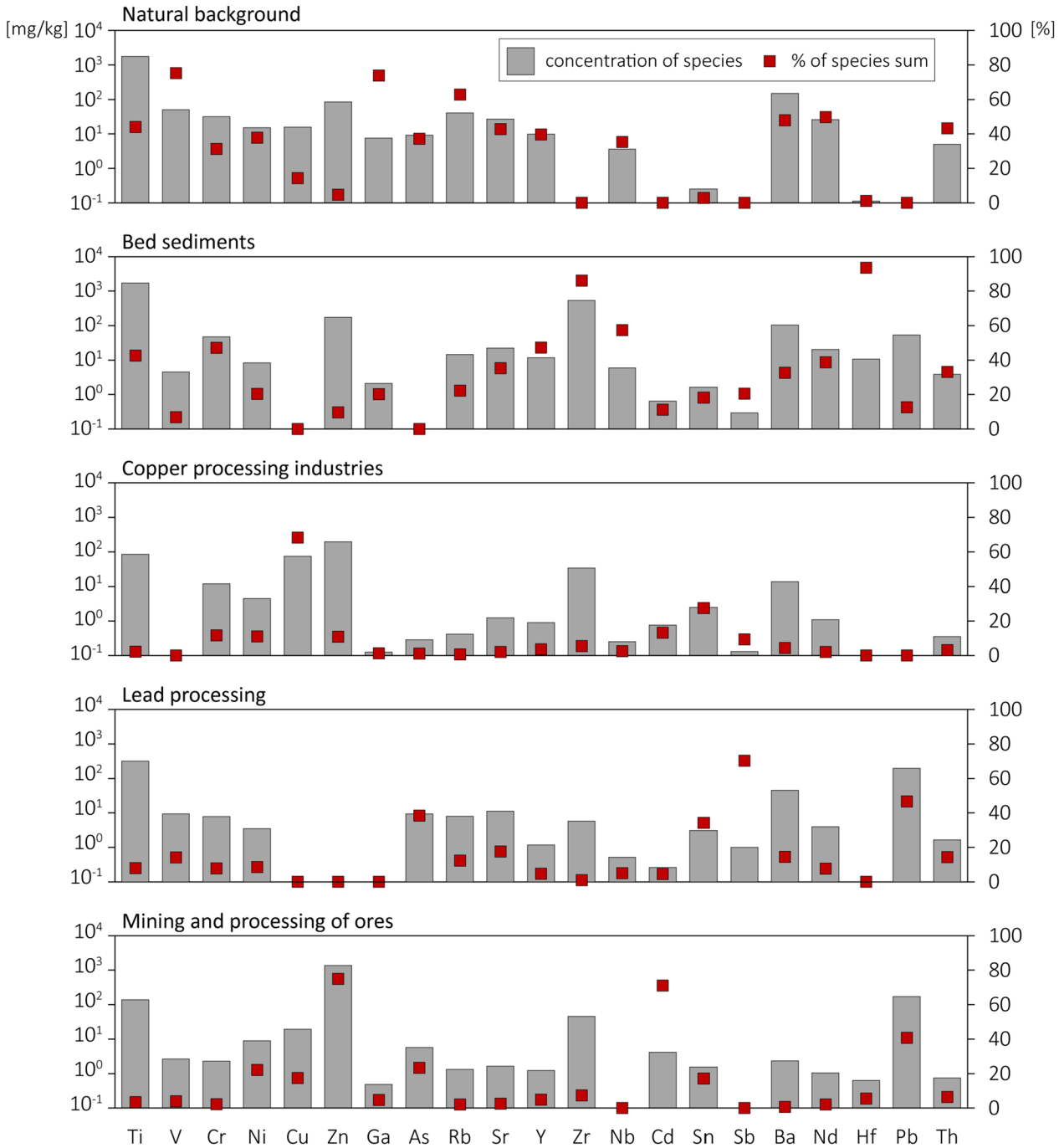

Fig. 8 Factor composition of the five factors identified by PMF. For details on factor identification, see text

with minor anthropogenic influence. This interpretation is supported by the absence of any apparent trend in this factor, either in different events or along the rivers (Figs. 10, 11).

Factor 2 is dominated by Hf and Zr, with 94% and 86% of their concentration, respectively, modeled by this factor. Further relevant elements include Nb, Y, Cr, Ti, Nd, Sr, Th, and Ba, with 57%, 47%, 47%, 43%, 39%, 35%, 33%, and 33%, respectively. The most abundant Zr mineral, by far, is zircon. Zircon and further resistant heavy minerals are enriched in stream sediments due to the naturally occurring sorting affecting fluvially transported sediment [152–154]. As the ionic radii of Zr and Hf are almost identical, the replacement of Zr atoms by Hf atoms in

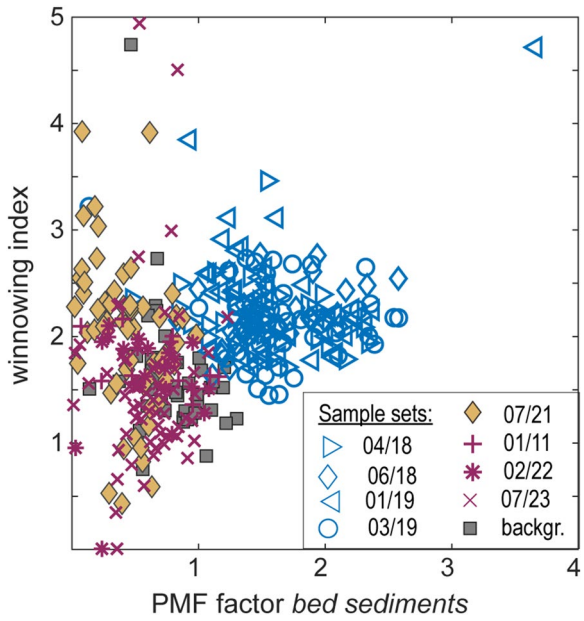

Fig. 9 The plot of factor contributions of PMF factor 2 against the winnowing index reveals a distinct positive relation. This supports the thesis that this PMF factor is formed by density-based sorting processes

Zr minerals is so common that all Zr minerals contain at least a small amount of Hf [152, 155, 156]. Hence, a strong correlation of their concentrations is expected. To a lesser extent, Zr is substituted by Nb and Y [156, 157]. Stream sediment is identified to have the highest median concentrations of Hf, Nd, Ti, and Zr among several sediment types [158, 159]. Zircon, rutile, and tourmaline are the typical heavy minerals enriched in weathered material derived from the Devonian slates in the study region [160–162]. Therefore, the high contribution of Ti to factor 2 can be linked to rutile, whereas the Cr content might be linked to tourmaline. The Eifel region is known for high Cr concentrations in bed sediments [158]. Li et al. [85] found Hf to indicate weathering in their PMF model.

The link between factor 2 and heavy minerals was tested using the winnowing index (WI) proposed by Grunsky et al. [145]. In this ratio, Al represents the lightweight clay fraction, whereas Th is supposed to indicate heavy minerals. Hence, a higher WI points toward the depletion of clay minerals and relative enrichment of heavy minerals, for example, due to winnowing processes. The relation between PMF factor 2 and the WI is depicted in Fig. 9. Higher contributions of factor 2 co-occur with an enhanced WI, thereby supporting the relevance of heavy minerals for this factor. However, there are some deviations from this connection for some samples, mainly of the flash flood event. As these samples are characterized by high factor contributions of the anthropogenic factors 3 to 5 (see below for the detailed description of the factors and Fig. S8 in the supplementary material for visualization), the enhanced Th concentrations in these samples might be linked to emissions of the metallurgical industries overflown during the extreme event. Altogether, factor 2 is interpreted to represent bed sediments impacted by hydrodynamic sorting. Detailed visualization and discussion of the impact of hydrodynamic sorting on factor 2 is provided in Fig. S10 in the supplementary material.

The remaining three factors have different characteristics, all containing only a few elements each. For **factor 3**, these are mainly Cu and Sn, with 68% and 28%, respectively. In addition, Cd, Cr, Ni, and Zn are of minor importance (13%, 12%, 11%, and 11%, respectively). Due to the occurrence of zinc ore in the region, Stolberg became a core area of the European brass industry in the nineteenth century. Some of these businesses have survived to this day and expanded their product palettes. Today, globally operating businesses produce a wide range of metallic products, including brass and bronze alloys with Cr, Zr, and Ni admixtures. Some companies use electroplating techniques, which require large basins in which the substances used, like Cu, Sn, Zn, or Ni, are present in dissolved form. Therefore, factor 3 is interpreted to represent brass industries and other copper processing plants.

Sb, Pb, As, and Sn constitute **factor 4**, with 70%, 47%, 38%, and 34% of them, respectively, being covered by this factor. Looking into absolute concentrations, lead dominates this factor. These compounds are typically linked to metallurgical industries [148, 163, 164]. The Stolberg region has a long history of lead processing. The emissions of the lead ore processing plants induced severe health issues in the local population, partly due to high lead concentrations in atmospheric dust fall-out [165, 166]. Interestingly, factor 4 exhibits some variances in the baseline sample set with slightly higher contributions in the Wehebach samples than in the samples taken at the upper Inde River (see Fig. S9 in the supplement). As both sample sets were taken from areas upstream of any industrial or settlement areas, fluvial input of these mainly anthropogenically emitted elements is unlikely. Instead, atmospheric deposition seems probable. As westerly winds dominate in this region, the Wehebach is located downwind from Stolberg, whereas the upper Inde River is in the opposite direction. Therefore, we assume factor 4 represents the lead processing industry, including direct inputs into the fluvial system and reworked atmospheric deposits.

Finally, 75% of Zn, 71% of Cd, and 41% of Pb are accounted for by **factor 5**. This factor contains smaller

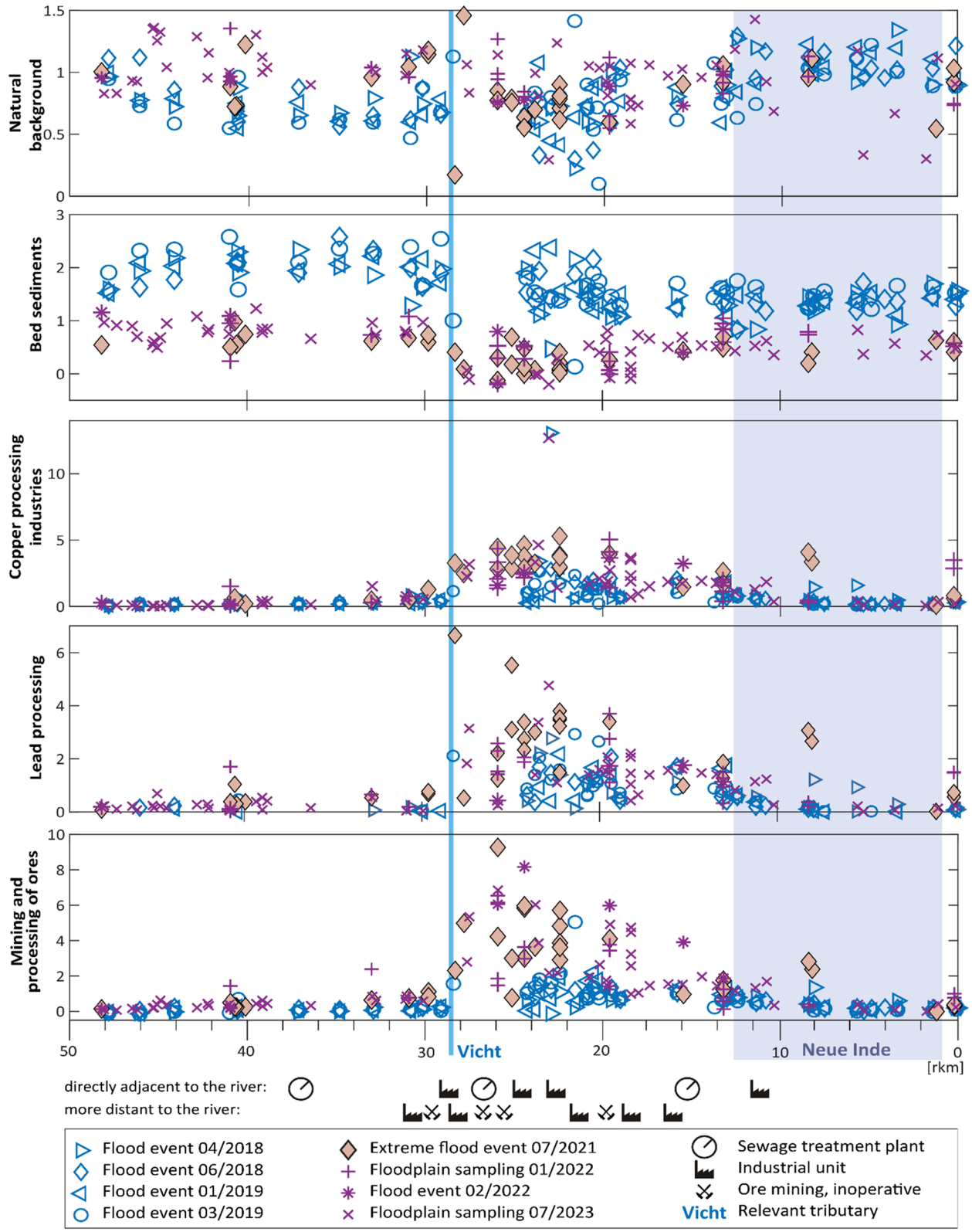

Fig. 10 Normalized factor contributions of five PMF factors along the Inde for the 8 investigated sample sets (the baseline set is excluded as it solely constitutes upstream samples). Emission-relevant land use in the proximate and distal floodplain is depicted below the x-axis. Furthermore, the mouth of the Vichtbach and the "Neue Inde" reach are located

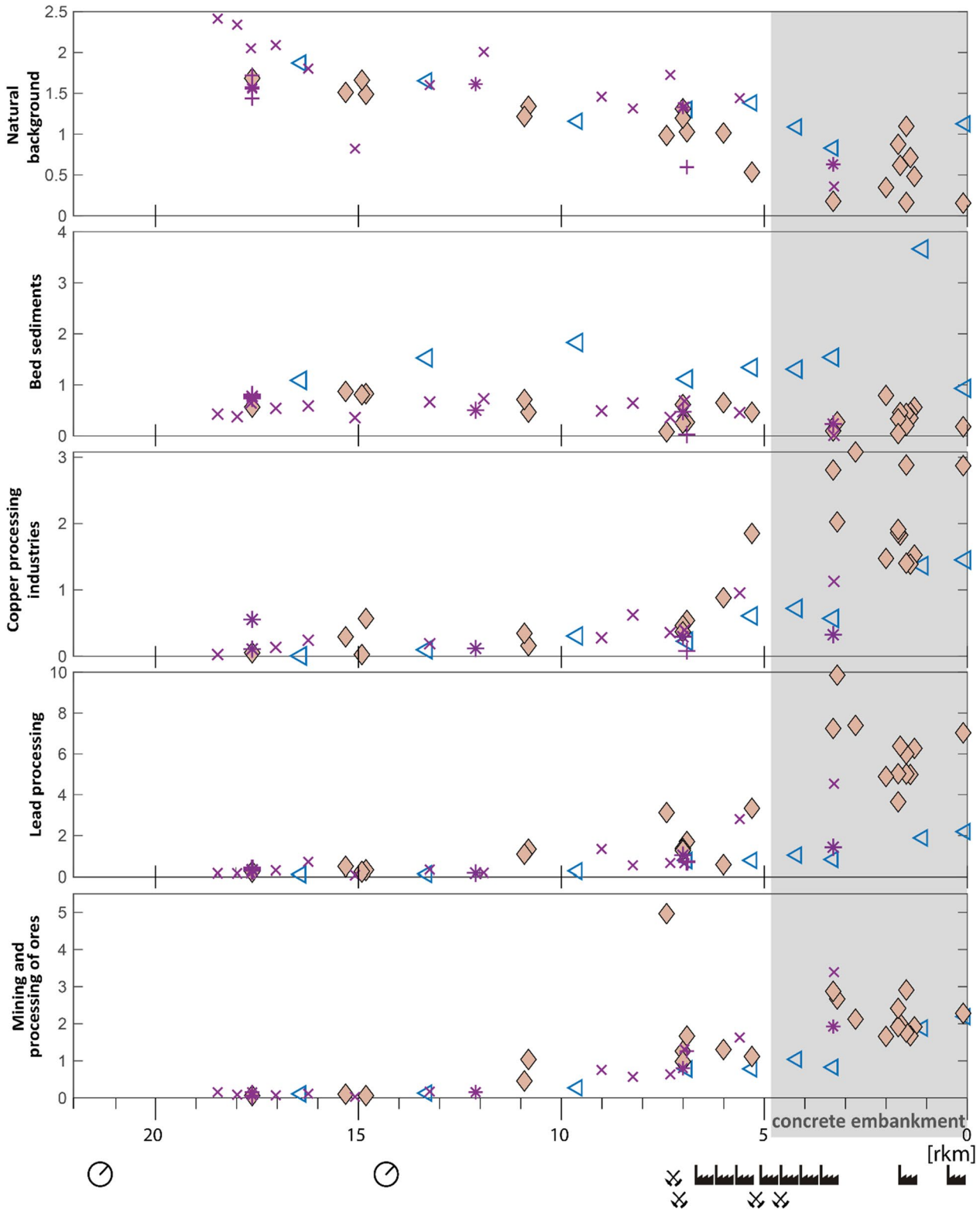

Fig. 11 Normalized factor contributions of all five factors along the Vichtbach for the 5 investigated sample sets (the floods in April 2018, June 2018, and March 2019 were not sampled along the Vichtbach). Emission-relevant land use in the proximate and distal floodplain is depicted below the x-axis. For details on illustrations, the reader is referred to the legend in Fig. 10

amounts of As, Ni, Cu, and Sn (23%, 22%, 18%, and 17%, respectively). The mining of Zn and Pb ores formerly dominated the region. These ores typically contained accessory amounts of further metals like Ni, Cu, As, Cd, and Sn [136]. Cd and Pb were found in several studies to accompany Zn ore mining and processing [81, 83, 86, 149, 167]. This factor exhibits a distinct "peak area" between the mouth of the Vichtbach and the city of Eschweiler. This area is known for a large number of brownfields. Therefore, factor 5 represents the legacy sediments of the former mining activities and the subsequent processing of the ores.

Spatial patterns of factor contributions

An analysis of the factors' characteristics during the different events and along the Inde and Vichtbach rivers was conducted based on factor contributions. This grouping is visualized in Figs. 10 and 11. Localizing unusual factor contributions can help identify specific emission sources, e.g., metal-processing industrial units, and may support the factors' identification.

The reaches with exceptionally high contributions in factors 3 to 5 coincide with the areas with intense industrial activity on the floodplains for both the Vichtbach and the Inde, thereby backing up the interpretation of these factors as related to anthropogenic emission sources. For both rivers, contributions of the anthropogenic factors are low upstream from the uppermost industrial units in the floodplains. Along the Vichtbach, contributions seem to grow constantly down to the mouth of the river. In the Inde River, the contributions of anthropogenic factors show a first marked increase from the Vichtbach mouth onward. However, even though there are many industrial units in the Inde floodplains in this reach, we found a slow but steady decrease in contributions of anthropogenic factors. When the "Neue Inde" is reached, factor contributions return to levels observed upstream of the industrial hotspots.

The two prominent outliers in the Cu-factor are both found in samples taken at the "Kupfermühlenkamp" which roughly translates to "Copper mill plot", indicating the processing of copper materials. However, the influence of these particles with exceptionally high copper contents is spatially very limited. A similar effect of locally strongly enhanced contributions can be seen for the ore mining factor that peaks at river kilometer (rkm) 7.4 of the Vichtbach (Fig. 11), which coincides with the uppermost former mining activity in the river's surroundings.

Comparing factor contributions in different events

Furthermore, comparing the different events allows for identifying the possible impact of the extreme event in July 2021. The following observations apply to both rivers. For the background factor, no apparent differences related to the extreme event were found. On the contrary, the second "natural factor" had distinctively higher contributions before the extreme event. Since the extreme event, factor contributions have been at a constant, lower level.

For all three "anthropogenic factors", a contrary trend with higher contributions in the aftermath of the event is evident. This does not apply to the upper reaches of Inde and Vichtbach, where contributions are generally low. The only exception is the ore mining factor, which shows a slight increase in the Inde River above the confluence of the Vichtbach since the extreme event. The input of trace elements from the Vichtbach into the Inde River necessarily shapes factor contributions from the confluence downwards. For all three anthropogenic factors, peak contributions for the extreme event and the consecutive data sets are much higher than for the sediments sampled before 2021. Along the Inde River, there is a downward trend in contributions that is especially distinct for the ore mining factor.

Discussion

Discharge dependency of trace element signatures in flood deposits

More regularly occurring flood events in northwestern European catchments are usually linked to steady rain over several days or snowmelt [19], both inducing slowly rising discharge in rivers. On the contrary, flash floods like the one in July 2021 are induced by extreme precipitation, leading to overland flow and inducing an unusually rapid discharge rise [104]. The resulting flood wave is steep, with very high water levels, widespread flooding, and outstanding stream power [106]. Therefore, sediment conveyance depends on the type of flooding. Recent studies found flash floods to be very effective transporting agents of suspended particulate matter and associated trace elements [168–170]. Differences in the trace elements load during extreme discharge events were found in mining-impacted catchments [16, 18, 171]. The particularly effective transport during flash floods also shaped the processes in the Inde catchment in July 2021.

For some elements, a marked drop to EF ≅ 1, i.e., baseline levels, from the flash flood onwards was found. This group (B.1) is dominated by elements that typically become enriched during weathering processes [172]. This indicates that the sediments stored within the river bed prior to the flash flooding that were subject to intense weathering were flushed out of the catchment, which hints at the abrogation of the sediment cascade that usually dominates the transport processes of flood sediments in any catchment. Further indication for this is found in

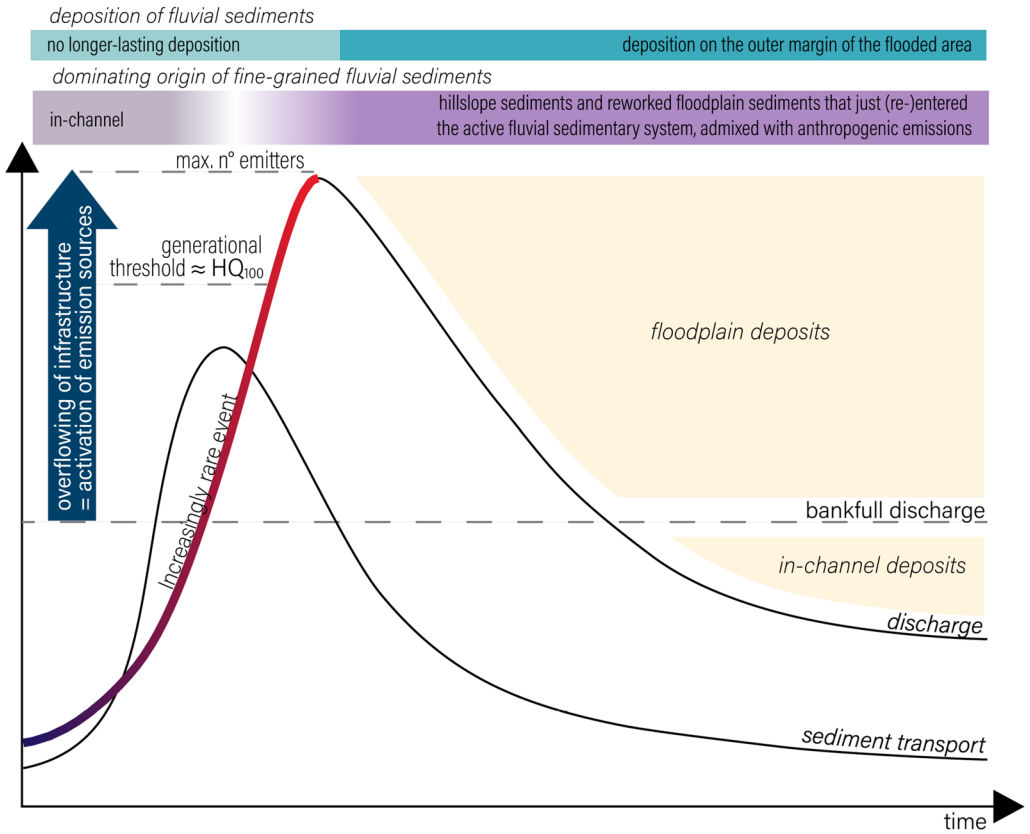

Fig. 12 Simplified visualization of the findings on sediment dynamics during flash flood events in gravel-dominated rivers. Discharge extremes result in high transport capacities, inducing a clockwise hysteresis of sediment transport. Hence, old channel sediments are completely flushed from the catchment, and flash flood deposits are rather dominated by 'fresh' sediments and anthropogenic impact due to the widespread flooding of unprotected infrastructure in the floodplains

the results of the PMF, which confirm the relevance of hydrodynamic sorting effects (for details on this see Fig. S10 in the supplementary material).

The slightly enhanced flow velocities of minor flood events are sufficient to entrain fine bed sediments up to small gravels. However, the transport capacity is not particularly high, so for sand and gravel only short-distance transport occurs, inducing deposition on nearby river banks and floodplains. This effect is evident for the sampled flood events in 2018 and 2019, which have higher contributions of the stream sediment factor. The striking decrease in this factor's contributions at the Inde River for all 2018 and 2019 events is related to changes in the riverbed's structure. From rkm 24 downwards, there is a drop in the roughness of the riverbed, which would be a prerequisite for effective sediment storage [173]. The artificial riverbed with minimized micro-scale structures lacks the potential for the retention of particles. Thus, there is a lower level of heavy minerals in the flood sediments (see Fig. 10). This abrupt change also implicates locally limited sediment transport during regular flood events, i.e., the sediment cascade is effective on short distances. Heavy particles tend to be transported via saltation, resulting in short-distance transport [173].

However, this observation does not apply to the flash flood: the contributions of factor 2 drop to a constantly lower level for all river reaches in the aftermath of the event, which points to the catchment-wide flushing of bed sediments. A short flushing effect at the onset of increasing runoff (Fig. 12) is generally acknowledged for all levels of flood events [39, 174]. This depletion of the stored fine sediments results in a clockwise hysteresis of fine-sediment concentration, typical for mid-European low mountain range rivers [175]. Usually, the declining gradient of rivers along their course causes a decrease in their velocity and, hence, their relative transport capacity, resulting in sedimentation in the case of sufficient material supply, thereby minimizing the flushing trend in lower catchments [176]. This is not only limited to floodplain deposits but also applies to in-channel sediments [176]. However, the minimal contributions of mature sediments along the complete river course since the

flash flood prove that the transport capacity during the extreme event was high enough to impede this process: the entire catchment was affected by such intensive erosion that all the fine sediments (< 2 mm) that were temporarily stored in the riverbed were flushed out.

In arid environments, the flushing effect of flash floods is documented to be so intense that all geochemical signals are reset back to baseline levels, including those influenced by anthropogenic input [170]. Siltation of riverbeds deteriorates the permeability of the bed [176], thereby inducing a multiplicity of negative ecological consequences [177]. In combination with the 'geochemical resetting', which implies approaching a more natural level of trace element concentrations, flash floods as a geomorphological process might benefit the riverine ecosystem.

However, this resetting character is disturbed by anthropogenic impact: the peaks of the anthropogenic PMF factors during the extreme event with a subsequent trend of slowly regressing contributions suggest emissions by sources that are solely activated above certain discharge thresholds (Fig. 12) that are not reached during regular flood events. As the Inde catchment is a former industrial hotspot, its floodplains are largely made up of sediments strongly enriched in elements related to these mining and industrial activities [136], and some of these legacy sites eroded during the extreme event [178]. The erosion of historically contaminated floodplain sediments is a well-known stressor for fluvial systems [1, 16, 179–185], and flash floods are particularly efficient erosional events [106]. Hence, extreme discharge events reactivate legacy sediments through erosion, whereas minor flood events transport present-day pollution [186]. The extensive dataset presented in this study supports the concern regarding the ongoing influence of mining legacies on catchments even decades after the last mine closed down [1]. Moreover, the overflowing of industrial areas during the extreme event contributed to concentration peaks, as seen from the extreme rise in levels of anthropogenic factors within Stolberg. Here, erosion is limited due to the river being fully channelized with concrete embankments, but industrial units located directly next to the river were hit hard by the flood.

Besides the erosion of contaminated sediments, leaching from water-saturated soils can promote enhanced concentrations of some trace elements in flood sediments [2, 16]. This effect needs some consideration because flash floods are oftentimes linked to antecedent saturation of soils [106, 187, 188]. Water saturation induces reducing conditions as soon as oxygen available to microorganisms is depleted. Microbial respiration switches to the reduction of iron, simultaneously mobilizing trace elements originally absorbed by this easily reducible iron. Upon re-oxidation, Fe and Mn-oxides form with a very high sorption capacity for further trace elements [111, 172, 189, 190]. Hence, water saturation in sediments can lead to the transport of trace elements from surrounding sediments to the channel, where they re-enter the active fluvial sedimentary system. Ciszewski & Grygar [14] argue that this process is only of minor importance for trace metal transfer from the floodplain to the channel compared to input via eroded bank sediments. However, erosion processes are restricted due to river engineering measures in the lower Inde catchment (i.e., by the trapezoidal cross-section of the river from Stolberg down to the "Neue Inde") [110]. Under high antecedent soil moisture, interflow was shown to be of particular relevance during flood events in Central European low mountain ranges [191]. In addition, receding water tables induce exfiltration of pore water from the banks [111]. Therefore, given the fact that the sorption of trace elements can take place within minutes or hours [111], their leaching from saturated soils seems plausible, but no statements on its relevance are possible.

In exploration geochemistry, it is standard practice to calculate the downstream dilution of a geochemical anomaly, i.e., outcropping ore bodies [120, 192]. The basic principle behind this idea can be transferred to point source pollution: without further input sources, trace element concentrations will be negatively correlated with the downstream distance from the source [5]. Hence, the downward decrease of the anthropogenic factors in the Inde indicates the absence of relevant additional input. Therefore, the onset of the downward trend at the upstream part of Eschweiler (Fig. 13) indicates that settlement areas are only of minor relevance as a source for anthropogenic trace metal(loid) input in the Inde catchment. The remarkably low contributions of anthropogenic factors in the "Neue Inde" are in accordance with other studies on this artificially-built river segment, which is built from uncontaminated, fresh sediment [193–195].

Like settlement areas, overflowing wastewater treatment plants were considered concerning pollution emitters. However, we found no proof of their relevance in terms of trace element pollution. Different sources becoming active at specific discharge levels, hence at different times within the event, will influence the respective chemical profile [27] and the spatial distribution of the emitted compounds in deposited sediments [16]. For example, compounds emitted by a source active solely in the earliest stages of the event have a high chance of being flushed from the catchment during the following higher stages of discharge. Therefore, the overflowing and flushing of the wastewater treatment plants that occurred early during the event might explain their low

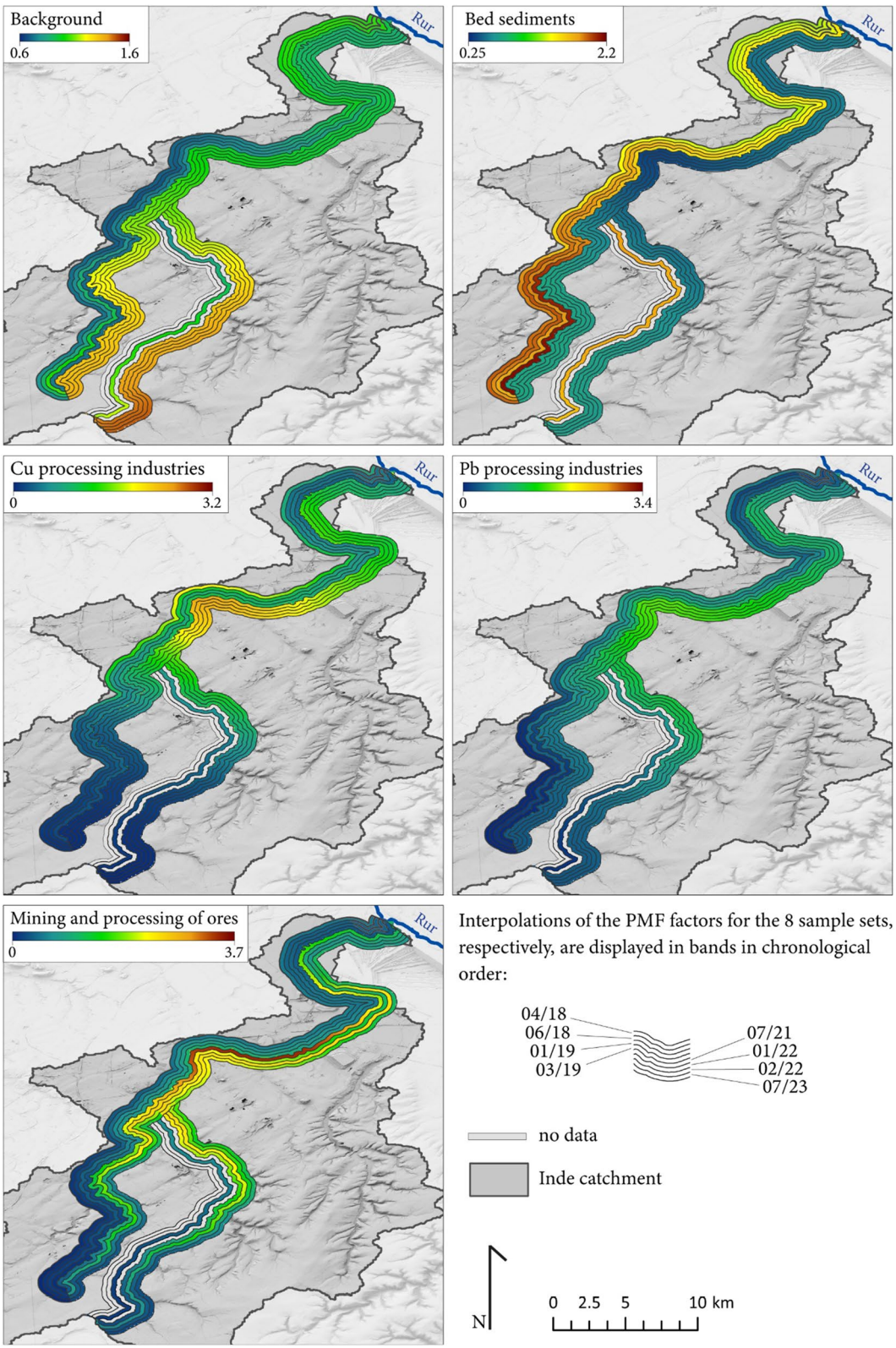

Fig. 13 Spatial interpolation of the five PMF factors for all sample sets. The interpolation was done using the Diffusion Interpolation with Barriers tool in ArcGIS using a DEM with 1 m resolution as a barrier feature. Each band represents a sample set, with the four on the left side of the river representing the 'before' and the four bands on the right side describing the situation since the flash flood. For the high-discharge events in 2018 and 2019, constant patterns are found. The flash flood induced a level change in factor contributions for all five factors

contributions to the trace element inventory in the flood deposits. This flushing is in agreement with the results found for the bed sediment factor.

However, the additional input of anthropogenically influenced risk elements during flood events depends on the specific situation of sources within the catchment and is, therefore, also discharge-dependent. High discharge (i.e., discharge events with a return period of > one generation, which strongly limits adaptative capacity) can lead to intense emission of anthropogenic pollution because of widespread flooding and because safety measures are not designed for this discharge level (Fig. 12). The "levee effect" leads to a calamitous sense of security [196] and promotes possibly hazardous land use in floodplains. Flash floods deserve special attention because of their perilous nature [197, 198] and because they are a dominating actor in sediment transport [171]. The likelihood of significantly enhanced concentrations of possible risk elements in sediments of extreme flood events adds up to these threats and demands a thorough public education on these risks [110]. Unfortunately, smaller catchments in rural areas, where oftentimes fewer flood protection measures are installed, are especially affected by flash floods [198].

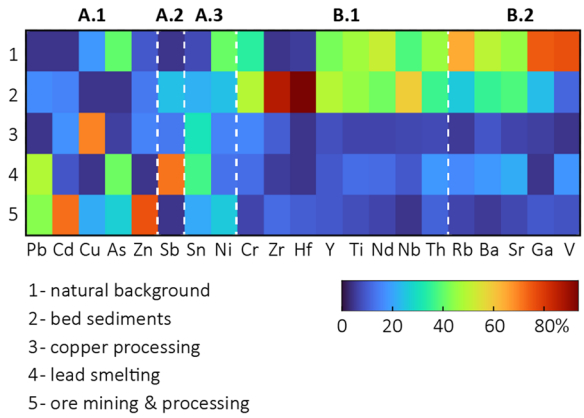

Fig. 14 Heatmap comparing the results obtained by investigating enrichment factors vs. PMF results. As denoted on the x-axis, the elements are sorted based on the grouping of elements as derived by EF (**A**—anthropogenically influenced, **B**–dominated by natural processes). The rows indicate the five PMF factors, and the color scheme visualizes the amount of each element covered by the respective factor. It becomes apparent that the results are similar. However, PMF provides a somewhat deeper and more differentiated understanding

The long-lasting impact of the extreme event on channel sediments

Differences in the pre-2021 floods, as identified by KW-testing, are limited to trace elements with EF close to 1. Deposits of regularly occurring floods seem to have unvarying trace element composition. For most trace elements, the flash flood disturbed this continuity. The system is expected to return to its old equilibrium state, as seen in the pre-2021 floods (see Fig. 13). However, no predictions on the duration of this can be made.

A clear downward trend was found for those trace elements enriched in the flash flood deposits (Pb, Cd, Cu, As, Zn), leading to the KW-test revealing that their enrichments are back to their respective pre-flash flood levels. This downward trend of anthropogenic factors is also found in the spatial interpolations of PMF factors (Fig. 13). However, the upper EF percentiles are still well above the 'before' values.

Flushing of weathered sediments from the channel was found; it is unclear how long it will take to rebuild the "old" status. Two years after the event, no trend can be observed. The high EF of Hf and Zr before the flash flood point at winnowing over a prolonged period.

PMF is a helpful tool in the analysis of flood sediments

By identifying patterns in trace element concentrations, PMF provided useful insights into flood sediment dynamics. In the vast majority of cases, when used to analyze sediments, only typical 'anthropogenic' heavy metals are used as input for PMF [143, 150, 199, 200]. By expanding the suite of trace elements used for the model, in addition to pollution emitters, PMF is also able to single out naturally driven processes like the winnowing of bed sediments. Further research addressing its suitability for provenance analysis in large-scale river systems seems worthwhile. First attempts have already been published [80, 85, 142, 164, 201], but the potential of this approach for sediment analysis does not yet appear to have been fully unlocked.

The general differentiation between elements dominated by natural processes and those mainly influenced by anthropogenic activities is found by analyzing enrichment factors corrected for baseline concentrations as well as by PMF (Fig. 14), which uses the original concentration data as input, supplemented by sample-specific uncertainty values. This aligns with other studies that found PMF to successfully differentiate between background factors and several anthropogenic factors [163]. The results obtained by the two approaches are in good agreement. However, only PMF, which extracts structural information on the interrelations of elements based on multidimensional data clouds [144], was able to identify differing sources for the anthropogenic elements. In contrast, comparing the distributions of EF is a strictly two-dimensional approach with the corresponding restrictions. Moreover, using PMF, the contribution of single elements to multiple sources (e.g., Pb) can be identified. This differentiation is not possible when relying

solely on the EF approach. In addition, PMF showed that Sn and Ni, which were classified as anthropogenic emissions, are not dominated by anthropogenic emissions. Rather, they appear to be part of natural sediment processes to the same extent (Fig. 14).

The modulated uncertainty calculation provided useful results. The results obtained were more stable than when common uncertainty calculation approaches were applied (for a list of commonly used uncertainty approaches, see [58]). As the uncertainty scaling is one of the key features of the PMF, its calculation should be considered duly and dataset-specific since it decides on the model's success [62, 66, 202, 203].

There are several reasons for preferring PMF over other multivariate statistical approaches, such as common FA or principal component analysis (PCA), when dealing with geochemical data. Common FA assumes 'random zero points' (like in social sciences, for example) and normally distributed data [55, 133, 204]; assumptions that the data presented here do not satisfy. FA and unscaled PCA are unduly influenced by large concentration values, which are a valid phenomenon in environmental sciences [66, 133]. Nevertheless, log transformations are an often followed approach to achieve normal distributions and limit the influence of high values. However, this destroys the model's linear structure while generating arbitrary power laws and can lead to spurious factors [133]. PCA (Q-mode and R-mode) was shown to be based on unrealistic error assumptions for the input data matrix when used in fields such as physics and chemistry [133, 140]. For both approaches, data transformations are necessary. However, centering the data is not advisable because it will inevitably lead to a loss of information when applied to geochemical data [133]. Autoscaling the original data was proven ineffective [134] and induces intensity ambiguity, meaning the solution is scale undetermined [205]. Furthermore, the ideal rank of the model depends on the scaling method applied [133].

Instead, PMF offers the unique feature of scaling the input matrix 'element-by-element' [133], ensuring optimal use of the information typically available in environmental sciences, like measurement uncertainties [88]. Therefore, no transformation of the input data is needed [73, 137, 205] so that information loss is avoided (regarding, e.g., the zero point of the data scale) [207]. PMF has been shown to provide results better fitting to the input data than FA or PCA approaches [59, 60, 62, 132, 206, 207]. While PCA performs under orthogonal constraints for the generated matrices, which results in solutions without actual physical meaning [132], PMF is based on a non-negativity constraint to enable the calculation of Eq. 2 [66], which leads to more meaningful results when applied in environmental sciences [58, 66, 73, 74, 88].

However, a certain level of expertise is required to evaluate the model's result. One frequently addressed drawback of PMF is that the algorithm will almost always provide a solution, leaving the user with the duty to identify misleading or erroneous results even though they might be hard to recognize [67, 208]. Hence, a thoughtful setup of the model and its parameters, including excessive examination of the results obtained using different model setups, is mandatory. For example, there is ongoing debate on how to determine the ideal number of factors [80].

Conclusions

Sediment deposits from flood events of different magnitudes and bank sediments were sampled over five years to investigate the effect of the discharge level on the trace element concentration in fluvial sediments.

For events with only slightly increased discharge, the transport capacity of the river does not exceed the sediment availability within the channel. Here, a locally limited sediment transport dominates, shaping the well-known fluvial sediment cascade. This state can be interpreted as a kind of equilibrium that is not disturbed by the aforementioned small flood events.

However, due to their exceptional stream power, flash floods generally induce flushing of the river's fine sediments with the potential to reset the geochemical signal. Such a resetting of the river bed sediments would be ecologically beneficial if the system were not disturbed by the additionally activated anthropogenic emission sources. High water levels, especially when combined with high flow velocities, induce overflowing and erosion in unexpected and, hence, unprotected areas. The material eroded here mixed with freshly eroded sediments from more natural areas forms the flood deposits found when waters receded. Consequently, the enrichment level of anthropogenic trace elements depends on the activated emission sources and, therefore, on the balance between discharge level and flow velocity on the one hand and flood protection measures on the other. However, location and type of sources are the main determining factors.

PMF based on a modified uncertainty calculation provided helpful results for identifying the sources influencing the trace element patterns in the fluvial sediments of the Inde. In addition to natural factors, current and past industrial activities were identified as controlling variables. The frequently expressed concern about emissions from sewage treatment plants and residential areas could not be substantiated for heavy metals in this study. Further investigations on the suitability of PMF for the analysis of sedimentary archives or for provenance analysis seem worthwhile.

In addition, further research is needed to investigate whether there is a direct relationship between transport distance and discharge or whether there is a certain threshold for catchment-wide flushing. Furthermore, the extent to which metals that are dissolved in the interflow and precipitate once they reach the active fluvial sedimentary system participate in elevated trace element levels is insufficiently known.

Abbreviations

PMF	Positive matrix factorization
HQ_x	Discharge for a flood event with a yearly reoccurrence probability of 1/x.
EF	Enrichment factor
KW-test	Kruskal Wallis test
XRF	X-Ray fluorescence
S/N	Signal-to-noise ratio
BS	Bootstrapping
DISP	Displacement
BS-DISP	Bootstrapping-displacement
rkm	River kilometre, starting from the river's mouth as rkm 0
FA	Factor analysis
PCA	Principal component analysis

Supplementary Information

The online version contains supplementary material available at https://doi.org/10.1186/s12302-024-00926-5.

Supplementary Material 1

Supplementary Material 2

Acknowledgements
First and foremost, we owe a great debt of gratitude to Verena Esser and Stefanie Wolf, who took samples from several flooding events in the Inde catchment for years and generated the valuable dataset this study is based on. A big thanks goes to Joana Jung, who conducted the extensive sampling of river banks in 2023. We appreciate the help in sampling by Carola Lehmkuhl, Philipp Schulte, Eva Vonden, Fabian Weichert, Piero Bellanova, Jan Schwarzbauer, Klaus Reicherter, Elena Klopries, and Janine Freyer. We thank Marianne Dohms and Renate Erdweg for the laboratory analysis. Julian Krieger's help in creating maps is appreciated. We thank Wolfgang Römer for his helpful comments on the manuscript. We are grateful for the financial support by the ABC/J Geoverbund, which supports the work of the HyCo-Geo Competence Centre. Furthermore, we acknowledge the financial support by the Deutsche Forschungsgemeinschaft and the RWTH Aachen University. We thank three anonymous reviewers for their helpful comments on an earlier manuscript version.

Author contributions
Conceptualization, AW; methodology; AW; sampling, AW, FL; data analysis, AW; writing-original draft preparation, AW; writing-review and editing, AW, FL; visualization, AW; supervision, FL; project administration, FL; funding acquisition, FL. All authors read and approved the final manuscript.

Funding
Open Access funding enabled and organized by Projekt DEAL. This work is supported by the Deutsche Forschungsgemeinschaft (DFG) under project numbers 496274914 and 418362535. Furthermore, the RWTH Aachen University supported our work by funding the project 'Projekthaus Wasser'. Publication fees were covered by the DEAL Initiative.

Availability of data and materials
The data presented in this study is provided in the supplementary information files. More detailed data on sampling location and measurement results are available from the corresponding author, AW, upon request.

Declarations

Ethics approval and consent to participate
Not applicable.

Consent for publication
Not applicable.

Competing interests
The authors declare that they have no competing interests.

Received: 6 March 2024 Accepted: 12 May 2024
Published online: 29 May 2024

References

1. Macklin MG, Thomas CJ, Mudbhatkal A, Brewer PA, Hudson-Edwards KA, Lewin J et al (2023) Impacts of metal mining on river systems: a global assessment. Science 381:1345–1350. https://doi.org/10.1126/science.adg6704
2. Byrne P, Wood PJ, Reid I (2012) The impairment of river systems by metal mine contamination: a review including remediation options. Crit Rev Environ Sci Technol 42:2017–2077. https://doi.org/10.1080/10643389.2011.574103
3. Coulthard TJ, Macklin MG (2003) Modeling long-term contamination in river systems from historical metal mining. Geol 31:451
4. Foulds SA, Brewer PA, Macklin MG, Haresign W, Betson RE, Rassner SME (2014) Flood-related contamination in catchments affected by historical metal mining: an unexpected and emerging hazard of climate change. Sci Total Environ 476–477:165–180. https://doi.org/10.1016/j.scitotenv.2013.12.079
5. Hudson-Edwards KA (2003) Sources, mineralogy, chemistry and fate ofheavy metal-bearing particles in mining-affected river systems. Mineral mag 67:205–217. https://doi.org/10.1180/0026461036720095
6. Bridge G (2004) Contested terrain: mining and the environment. Annu Rev Environ Resour 29:205–259. https://doi.org/10.1146/annurev.energy.28.011503.163434
7. Best J (2019) Anthropogenic stresses on the world's big rivers. Nature Geosci 12:7–21. https://doi.org/10.1038/s41561-018-0262-x
8. Csavina J, Field J, Taylor MP, Gao S, Landázuri A, Betterton EA, Sáez AE (2012) A review on the importance of metals and metalloids in atmospheric dust and aerosol from mining operations. Sci Total Environ 433:58–73. https://doi.org/10.1016/j.scitotenv.2012.06.013
9. Debnath A, Singh PK, Chandra Sharma Y (2021) Metallic contamination of global river sediments and latest developments for their remediation. J Environ Manage 298:113378. https://doi.org/10.1016/j.jenvman.2021.113378
10. Förstner U, Müller G (1973) Heavy metal accumulation in river sediments: a response to environmental pollution. Geoforum 4:53–61. https://doi.org/10.1016/0016-7185(73)90006-7
11. Foster IDL, Charlesworth SM (1996) Heavy metals in the hydrological cycle: trends and explanation. Hydrol Process 10:227–261
12. Ali H, Khan E, Ilahi I (2019) Environmental chemistry and ecotoxicology of hazardous heavy metals: environmental persistence, toxicity, and bioaccumulation. J Chem 2019:1–14. https://doi.org/10.1155/2019/6730305
13. Ersoy A (2021) Critical review of the environmental investigation on soil heavy metal contamination. Appl Ecol Env Res 19:3853–3878. https://doi.org/10.15666/aeer/1905_38533878
14. Ciszewski D, Grygar TM (2016) A review of flood-related storage and remobilization of heavy metal pollutants in river systems. Water Air Soil Pollut 227:239. https://doi.org/10.1007/s11270-016-2934-8
15. Cánovas CR, Olías M, Sarmiento AM, Nieto JM, Galván L (2012) Pollutant transport processes in the Odiel River (SW Spain) during rain events. Water Resour Res. https://doi.org/10.1029/2011WR011041
16. Resongles E, Casiot C, Freydier R, Le Gall M, Elbaz-Poulichet F (2015) Variation of dissolved and particulate metal(loid) (As, Cd, Pb, Sb, Tl, Zn) concentrations under varying discharge during a mediterranean flood

in a former mining watershed, the Gardon River (France). J Geochem Explor 158:132–142. https://doi.org/10.1016/j.gexplo.2015.07.010
17. Bábek O, Faměra M, Hilscherová K, Kalvoda J, Dobrovolný P, Sedláček J et al (2011) Geochemical traces of flood layers in the fluvial sedimentary archive; implications for contamination history analyses. CATENA 87:281–290. https://doi.org/10.1016/j.catena.2011.06.014
18. Dhivert E, Grosbois C, Coynel A, Lefèvre I, Desmet M (2015) Influences of major flood sediment inputs on sedimentary and geochemical signals archived in a reservoir core (Upper Loire Basin, France). CATENA 126:75–85. https://doi.org/10.1016/j.catena.2014.10.030
19. Blöschl G, Hall J, Viglione A, Perdigão RAP, Parajka J, Merz B et al (2019) Changing climate both increases and decreases European river floods. Nature 573:108–111. https://doi.org/10.1038/s41586-019-1495-6
20. Milly PCD, Wetherald RT, Dunne KA, Delworth TL (2002) Increasing risk of great floods in a changing climate. Nature 415:514–517. https://doi.org/10.1038/415514a
21. Tellman B, Sullivan JA, Kuhn C, Kettner AJ, Doyle CS, Brakenridge GR et al (2021) Satellite imaging reveals increased proportion of population exposed to floods. Nature 596:80–86. https://doi.org/10.1038/s41586-021-03695-w
22. Rentschler J, Salhab M, Jafino BA (2022) Flood exposure and poverty in 188 countries. Nat Commun 13:3527. https://doi.org/10.1038/s41467-022-30727-4
23. Mazzoleni M, Mård J, Rusca M, Odongo V, Lindersson S, Di Baldassarre G (2021) Floodplains in the Anthropocene: a global analysis of the interplay between human population, built environment, and flood severity. Water Res. https://doi.org/10.1029/2020WR027744
24. Andreadis KM, Wing OEJ, Colven E, Gleason CJ, Bates PD, Brown CM (2022) Urbanizing the floodplain: global changes of imperviousness in flood-prone areas. Environ Res Lett 17:104024. https://doi.org/10.1088/1748-9326/ac9197
25. Best J, Ashmore P, Darby SE (2022) Beyond just floodwater. Nat Sustain 5:811–813. https://doi.org/10.1038/s41893-022-00929-1
26. Ciszewski D (2001) Flood-related changes in heavy metal concentrations within sediments of the Biaa Przemsza River. Geomorphology 40:205–218. https://doi.org/10.1016/S0169-555X(01)00044-7
27. Coynel A, Schäfer J, Blanc G, Bossy C (2007) Scenario of particulate trace metal and metalloid transport during a major flood event inferred from transient geochemical signals. Appl Geochem 22:821–836. https://doi.org/10.1016/j.apgeochem.2006.10.004
28. Lehmann J, Puff T, Damke H, Eidam J, Henning K-H, Jülich W-D, Roßberg H (1999) The Odra River load of heavy metals at hohenwutzen during the flood in 1997. Acta hydrochim hydrobiol 27:321–324
29. Lintern A, Leahy PJ, Heijnis H, Zawadzki A, Gadd P, Jacobsen G et al (2016) Identifying heavy metal levels in historical flood water deposits using sediment cores. Water Res 105:34–46. https://doi.org/10.1016/j.watres.2016.08.041
30. Tobin GA, Brinkmann R, Montz BE (2000) Flooding and the distribution of selected metals in floodplain sediments in St. Maries Idaho. Environ Geochem Health 22:219–232. https://doi.org/10.1023/A:1026502324603
31. Crawford SE, Brinkmann M, Ouellet JD, Lehmkuhl F, Reicherter K, Schwarzbauer J et al (2022) Remobilization of pollutants during extreme flood events poses severe risks to human and environmental health. J Hazard Mater 421:126691. https://doi.org/10.1016/j.jhazmat.2021.126691
32. Čmelík J, Brovdyová T, Trögl J, Neruda M, Kadlečík M, Pacina J et al (2019) Changes in the content of heavy metals in Bílina river during 2012–2017: effects of flood and industrial inputs. Water 11:481. https://doi.org/10.3390/w11030481
33. Dennis IA, Macklin MG, Coulthard TJ, Brewer PA (2003) The impact of the october-november 2000 floods on contaminant metal dispersal in the river swale catchment, North Yorkshire. UK Hydrol Process 17:1641–1657. https://doi.org/10.1002/hyp.1206
34. Runkel RL, Kimball BA, Nimick DA, Walton-Day K (2016) Effects of flow regime on metal concentrations and the attainment of water quality standards in a remediated stream reach, butte Montana. Environ Sci Technol 50:12641–12649. https://doi.org/10.1021/acs.est.6b03190
35. Antić-Mladenović S, Kresović M, Čakmak D, Perović V, Saljnikov E, Ličina V, Rinklebe J (2019) Impact of a severe flood on large-scale contamination of arable soils by potentially toxic elements (Serbia). Environ Geochem Health 41:249–266. https://doi.org/10.1007/s10653-018-0138-4
36. Pulley S, Foster I, Antunes P (2016) The dynamics of sediment-associated contaminants over a transition from drought to multiple flood events in a lowland UK catchment. Hydrol Process 30:704–719. https://doi.org/10.1002/hyp.10616
37. Hilscherova K, Dusek L, Kubik V, Cupr P, Hofman J, Klanova J, Holoubek I (2007) Redistribution of organic pollutants in river sediments and alluvial soils related to major floods. J Soils Sediments 7:167–177. https://doi.org/10.1065/jss2007.04.222
38. Hurley R, Woodward J, Rothwell JJ (2018) Microplastic contamination of river beds significantly reduced by catchment-wide flooding. Nature Geosci 11:251–257. https://doi.org/10.1038/s41561-018-0080-1
39. Bradley SB, Lewin J (1982) Transport of heavy metals on suspended sediments under high flow conditions in a mineralised region of wales. Environ Pollut B 4:257–267. https://doi.org/10.1016/0143-148X(82)90012-X
40. Dawson EJ, Macklin MG (1998) Speciation of heavy metals on suspended sediment under high flow conditions in the River Aire, West Yorkshire. UK Hydrol Process 12:1483–1494
41. Zhang L, Zhang Z, Chen Y, Fu Y (2015) Sediment characteristics, floods, and heavy metal pollution recorded in an overbank core from the lower reaches of the Yangtze River. Environ Earth Sci 74:7451–7465. https://doi.org/10.1007/s12665-015-4733-8
42. Žák K, Rohovec J, Navrátil T (2009) Fluxes of heavy metals from a highly polluted watershed during flood events: a case study of the Litavka River, Czech Republic. Water Air Soil Pollut 203:343–358. https://doi.org/10.1007/s11270-009-0017-9
43. Zerling L, Hanisch C, Junge FW (2006) Heavy metal inflow into the floodplains at the mouth of the river Weiße Elster (Central Germany). Acta hydrochim hydrobiol 34:234–244. https://doi.org/10.1002/aheh.200400624
44. Talská R, Hron K, Grygar TM (2021) Compositional scalar-on-function regression with application to sediment particle size distributions. Math Geosci 53:1667–1695. https://doi.org/10.1007/s11004-021-09941-1
45. Filzmoser P, Hron K, Reimann C (2009) Univariate statistical analysis of environmental (compositional) data: problems and possibilities. Sci Total Environ 407:6100–6108. https://doi.org/10.1016/j.scitotenv.2009.08.008
46. Álvarez-Vázquez MÁ, Hošek M, Elznicová J, Pacina J, Hron K, Fačevicová K et al (2020) Separation of geochemical signals in fluvial sediments: new approaches to grain-size control and anthropogenic contamination. Appl Geochem. https://doi.org/10.1016/j.apgeochem.2020.104791
47. Matys Grygar T, Popelka J (2016) Revisiting geochemical methods of distinguishing natural concentrations and pollution by risk elements in fluvial sediments. J Geochem Explor 170:39–57. https://doi.org/10.1016/j.gexplo.2016.08.003
48. Tůmová Š, Hrubešová D, Vorm P, Hošek M, Grygar TM (2019) Common flaws in the analysis of river sediments polluted by risk elements and how to avoid them: case study in the Ploučnice River system, Czech republic. J Soils Sediment 19:2020–2033. https://doi.org/10.1007/s11368-018-2215-9
49. Bábek O, Grygar TM, Faměra M, Hron K, Nováková T, Sedláček J (2015) Geochemical background in polluted river sediments: how to separate the effects of sediment provenance and grain size with statistical rigour? CATENA 135:240–253. https://doi.org/10.1016/j.catena.2015.07.003
50. Loring DH (1991) Normalization of heavy-metal data from estuarine and coastal sediments. ICES J Mar Sci 48:101–115. https://doi.org/10.1093/icesjms/48.1.101
51. Matys Grygar T (2022) Comment to Ballasus et al. (2022). Sci Total Environ. https://doi.org/10.1016/j.scitotenv.2022.155371
52. Matys Grygar T, Elznicová J, Tůmová Š, Kylich T, Skála J, Hron K, Álvarez-Vázquez MÁ (2023) Moving from geochemical to contamination maps using incomplete chemical information from long-term high-density monitoring of Czech agricultural soils. Environ Earth Sci. https://doi.org/10.1007/s12665-022-10692-3
53. Faměra M, Matys Grygar T, Ciszewski D, Czajka A, Álvarez-Vázquez MÁ, Hron K et al (2021) Anthropogenic records in a fluvial depositional system: the odra river along the Czech-polish border. Anthropocene. https://doi.org/10.1016/j.ancene.2021.100286

54. Schlumberger J, Haasnoot M, Aerts J, de Ruiter M (2022) Proposing DAPP-MR as a disaster risk management pathways framework for complex, dynamic multi-risk. I Science. https://doi.org/10.1016/j.isci.2022.105219
55. Dupont MF, Elbourne A, Cozzolino D, Chapman J, Truong VK, Crawford RJ, Latham K (2020) Chemometrics for environmental monitoring: a review. Anal Methods 12:4597–4620. https://doi.org/10.1039/D0AY01389G
56. Hopke PK (2016) Review of receptor modeling methods for source apportionment. J Air Waste Manag Assoc 66:237–259. https://doi.org/10.1080/10962247.2016.1140693
57. Chen H, Teng Y, Li J, Wu J, Wang J (2016) Source apportionment of trace metals in river sediments: a comparison of three methods. Environ Pollut 211:28–37. https://doi.org/10.1016/j.envpol.2015.12.037
58. Reff A, Eberly SI, Bhave PV (2007) Receptor modeling of ambient particulate matter data using positive matrix factorization: review of existing methods. J Air Waste Manag Assoc 57:146–154. https://doi.org/10.1080/10473289.2007.10465319
59. Salim I, Sajjad RU, Paule-Mercado MC, Memon SA, Lee B-Y, Sukhbaatar C, Lee C-H (2019) Comparison of two receptor models PCA-MLR and PMF for source identification and apportionment of pollution carried by runoff from catchment and sub-watershed areas with mixed land cover in South Korea. Sci Total Environ 663:764–775. https://doi.org/10.1016/j.scitotenv.2019.01.377
60. Miller SL, Anderson MJ, Daly EP, Milford JB (2002) Source apportionment of exposures to volatile organic compounds I. evaluation of receptor models using simulated exposure data. Atmos Environ 36:3629–3641. https://doi.org/10.1016/S1352-2310(02)00279-0
61. Belis CA, Karagulian F, Amato F, Almeida M, Artaxo P, Beddows D et al (2015) A new methodology to assess the performance and uncertainty of source apportionment models II: the results of two European intercomparison exercises. Atmos Environ 123:240–250. https://doi.org/10.1016/j.atmosenv.2015.10.068
62. Pekey H, Doğan G (2013) Application of positive matrix factorisation for the source apportionment of heavy metals in sediments: a comparison with a previous factor analysis study. Microchem J 106:233–237. https://doi.org/10.1016/j.microc.2012.07.007
63. Tauler R, Viana M, Querol X, Alastuey A, Flight RM, Wentzell PD, Hopke PK (2009) Comparison of the results obtained by four receptor modelling methods in aerosol source apportionment studies. Atmos Environ 43:3989–3997. https://doi.org/10.1016/j.atmosenv.2009.05.018
64. Bzdusek PA, Christensen ER (2006) Comparison of a new variant of PMF with other receptor modeling methods using artificial and real sediment PCB data sets. Environmetrics 17:387–403. https://doi.org/10.1002/env.777
65. Diakite ML, Hu Y, Cheng H (2021) Source apportionment based on the comparative approach of two receptor models in a large-scale region in China. Environ Sci Pollut Res Int 28:56696–56710. https://doi.org/10.1007/s11356-021-14602-1
66. Paatero P, Tapper U (1994) Positive matrix factorization: a non-negative factor model with optimal utilization of error estimates of data values. Environmetrics 5:111–126. https://doi.org/10.1002/env.3170050203
67. Ulbrich IM, Canagaratna MR, Zhang Q, Worsnop DR, Jimenez JL (2009) Interpretation of organic components from positive matrix factorization of aerosol mass spectrometric data. Atmos Chem Phys 9:2891–2918. https://doi.org/10.5194/acp-9-2891-2009
68. Kim E, Hopke PK (2005) Improving source apportionment of fine particles in the eastern United States utilizing temperature-resolved carbon fractions. J Air Waste Manag Assoc 55:1456–1463. https://doi.org/10.1080/10473289.2005.10464748
69. Brown SG, Frankel A, Raffuse SM, Roberts PT, Hafner HR, Anderson DJ (2007) Source apportionment of fine particulate matter in phoenix, AZ, using positive matrix factorization. J Air Waste Manag Assoc 57:741–752. https://doi.org/10.3155/1047-3289.57.6.741
70. Polissar AV, Hopke PK, Paatero P, Malm WC, Sisler JF (1998) Atmospheric aerosol over Alaska: 2. elemental composition and sources. J Geophys Res 103:19045–19057. https://doi.org/10.1029/98JD01212
71. Chan Y, Hawas O, Hawker D, Vowles P, Cohen DD, Stelcer E et al (2011) Using multiple type composition data and wind data in PMF analysis to apportion and locate sources of air pollutants. Atmos Environ 45:439–449. https://doi.org/10.1016/j.atmosenv.2010.09.060
72. Kim E, Hopke PK, Edgerton ES (2004) Improving source identification of atlanta aerosol using temperature resolved carbon fractions in positive matrix factorization. Atmos Environ 38:3349–3362. https://doi.org/10.1016/j.atmosenv.2004.03.012
73. Lee E, Chan CK, Paatero P (1999) Application of positive matrix factorization in source apportionment of particulate pollutants in Hong Kong. Atmos Environ 33:3201–3212. https://doi.org/10.1016/S1352-2310(99)00113-2
74. Paterson KG, Sagady JL, Hooper DL, Bertman SB, Carroll MA, Shepson PB (1999) Analysis of air quality data using positive matrix factorization. Environ Sci Technol 33:635–641. https://doi.org/10.1021/es980605j
75. Buzcu B, Fraser MP (2006) Source identification and apportionment of volatile organic compounds in Houston, TX. Atmos Environ 40:2385–2400. https://doi.org/10.1016/j.atmosenv.2005.12.020
76. Schauer JJ, Cass GR (2000) Source apportionment of wintertime gas-phase and particle-phase air pollutants using organic compounds as tracers. Environ Sci Technol 34:1821–1832. https://doi.org/10.1021/es981312t
77. Chaturvedi R, Das B, Banerjee S, Bhattacharjee CR (2020) Groundwater quality characterization of north brahmaputra basin using positive matrix factorization. Phys Sci. https://doi.org/10.1007/s40010-020-00712-x
78. Celen M, Oruc HN, Adiller A, Yıldız Töre G, Onkal Engin G (2022) Contribution for pollution sources and their assessment in urban and industrial sites of Ergene River Basin. Turkey Int J Environ Sci Technol 19:11789–11808. https://doi.org/10.1007/s13762-022-03919-0
79. Alves DD, Riegel RP, de Quevedo DM, Osório DMM, Da Costa GM, do Nascimento CA, Telöken F (2018) Seasonal assessment and apportionment of surface water pollution using multivariate statistical methods: Sinos River, southern Brazil. Environ Monit Assess 190:384. https://doi.org/10.1007/s10661-018-6759-3
80. Saylor JE, Sundell KE, Sharman GR (2019) Characterizing sediment sources by non-negative matrix factorization of detrital geochronological data. Earth Planet Sci Lett 512:46–58. https://doi.org/10.1016/j.epsl.2019.01.044
81. González-Macías C, Sánchez-Reyna G, Salazar-Coria L, Schifter I (2014) Application of the positive matrix factorization approach to identify heavy metal sources in sediments. a case study on the mexican Pacific Coast. Environ Monit Assess 186:307–324. https://doi.org/10.1007/s10661-013-3375-0
82. Vaccaro S, Sobiecka E, Contini S, Locoro G, Free G, Gawlik BM (2007) The application of positive matrix factorization in the analysis, characterisation and detection of contaminated soils. Chemosphere 69:1055–1063. https://doi.org/10.1016/j.chemosphere.2007.04.032
83. Comero S, Locoro G, Free G, Vaccaro S, de Capitani L, Gawlik BM (2011) Characterisation of Alpine lake sediments using multivariate statistical techniques. Chemom Intell Lab Syst 107:24–30. https://doi.org/10.1016/j.chemolab.2011.01.002
84. Comero S, Servida D, de Capitani L, Gawlik BM (2012) Geochemical characterization of an abandoned mine site: a combined positive matrix factorization and GIS approach compared with principal component analysis. J Geochem Explor 118:30–37. https://doi.org/10.1016/j.gexplo.2012.04.003
85. Li T, Li X, Luo W, Cai G (2019) Combined classification and source apportionment analysis for trace elements in western Philippine Sea sediments. Sci Total Environ 675:408–419. https://doi.org/10.1016/j.scitotenv.2019.04.236
86. Chen Z, Ding Y, Jiang X, Duan H, Ruan X, Li Z, Li Y (2022) Combination of UNMIX, PMF model and Pb-Zn-Cu isotopic compositions for quantitative source apportionment of heavy metals in suburban agricultural soils. Ecotoxicol Environ Saf. https://doi.org/10.1016/j.ecoenv.2022.113369
87. Xia F, Zhang C, Qu L, Song Q, Ji X, Mei K et al (2020) A comprehensive analysis and source apportionment of metals in riverine sediments of a rural-urban watershed. J Hazard Mater. https://doi.org/10.1016/j.jhazmat.2019.121230
88. Paatero P (1997) Least squares formulation of robust non-negative factor analysis. Chemom Intell Lab Syst 37:23–35. https://doi.org/10.1016/S0169-7439(96)00044-5
89. Norris G, Duvall R, Brown SG (2014) EPA positive matrix factorization (PMF) 50. Fundamentals and user guide, Washington

90. Land NRW Stammdaten Pegel Eschweiler. 2023. https://www.elwasweb.nrw.de/elwas-web/index.xhtml.
91. Schmidt-Wygasch C. Neue Untersuchungen zur holozänen Genese des Unterlaufs der Inde: chronostratigraphische Differenzierung der Auelehme unter besonderer Berücksichtigung der Montangeschichte der Voreifel. Dissertation, Aachen: RWTH Aachen University. 2011
92. Paul J. Grenzen der Belastbarkeit: Die Flüsse Rur (Roer) und Inde im Industriezeitalter. Joseph-Kuhl-Ges, Jülich. 1994
93. Esser V. Investigations on fluvial morphodynamics and recent pollutant dispersion in river systems—examples from the border region of Belgium, the Netherlands and Germany. Dissertation, Aachen: RWTH Aachen University. 2020
94. Sindern S, Görtz A, Gronen L (2016) Historic and recent anthropogenic emissions of heavy metals in the town of Stolberg (Rhine area, Germany). Jber oberrh 98:15–31. https://doi.org/10.1127/jmogv/98/0003
95. Offermanns H (2019) Messing—konfliktstoff im aachener raum. Chemie in nserer Zeit 53:263–265. https://doi.org/10.1002/ciuz.201900871
96. Struck BD, Froning M, Pelzer R, Sistemich I, Ostapezuk P (1996) Atmospheric dispersion and physicochemical behaviour of Cd and Pb in rainwater after emission by a lead works. Sci Total Environ 182:85–91. https://doi.org/10.1016/0048-9697(96)05055-3
97. Tradowsky JS, Philip SY, Kreienkamp F, Kew SF, Lorenz P, Arrighi J et al (2023) Attribution of the heavy rainfall events leading to severe flooding in Western Europe during july 2021. Clim Change. https://doi.org/10.1007/s10584-023-03502-7
98. Lehmkuhl F, Schüttrumpf H, Schwarzbauer J, Brüll C, Dietze M, Letmathe P et al (2022) Assessment of the 2021 summer flood in central Europe. Environ Sci Eur. https://doi.org/10.1186/s12302-022-00685-1
99. Belleflamme A, Goergen K, Iakunin M, Vanderborght J, Kollet S. The extreme flood events of summer 2021 in western Germany and Belgium as simulated by the free-running ParFlow hydrological model. 2021
100. Schäfer A, Mühr B, Daniell J, Ehret U, Ehmele F, Küpfer K, et al. (2021) Hochwasser Mitteleuropa, Juli 2021 (Deutschland) : 21. Juli 2021 – Bericht Nr. 1 „Nordrhein-Westfalen & Rheinland-Pfalz". Karlsruher Institut für Technologie (KIT).
101. Junghänel T, Bissolli P, Daßler J, Fleckenstein R, Imbery F, Janssen W, et al. 2021. Hydro-klimatische Einordnung der Stark- und Dauerniederschläge in Teilen Deutschlands im Zusammenhang mit dem Tiefdruckgebiet. "Bernd". 12(19).
102. Mohr S, Ehret U, Kunz M, Ludwig P, Caldas-Alvarez A, Daniell JE et al (2023) A multi-disciplinary analysis of the exceptional flood event of july 2021 in central Europe—part 1: event description and analysis. Nat Hazards Earth Syst Sci 23:525–551. https://doi.org/10.5194/nhess-23-525-2023
103. Kreienkamp F, Philip SY, Tradowsky JS, Kew SF, Lorenz P, Arrighi J et al (2021) Rapid attribution of heavy rainfall events leading to the severe flooding in Western Europe during July. World Weather Atribution 2:51–55
104. Dietze M, Bell R, Ozturk U, Cook KL, Andermann C, Beer AR et al (2022) More than heavy rain turning into fast-flowing water—a landscape perspective on the 2021 Eifel floods. Nat Hazards Earth Syst Sci 22:1845–1856. https://doi.org/10.5194/nhess-22-1845-2022
105. Dietze M, Ozturk U (2021) A flood of disaster response challenges. Science 373:1317–1318. https://doi.org/10.1126/science.abm0617
106. Bronstert A, Crisologo I, Heistermann M, Ozturk U, Vogel K, Wendi D (2020) Flash-floods: more often, more severe, more damaging? An analysis of hydro-geo-environmental conditions and anthropogenic impacts. In: Leal Filho W, Nagy GJ, Borga M, Chávez Muñoz PD, Magnuszewski A (eds) Climate change, hazards and adaptation options. Springer International Publishing, Cham, pp 225–244
107. Ludwig P, Ehmele F, Franca MJ, Mohr S, Caldas-Alvarez A, Daniell JE et al (2023) A multi-disciplinary analysis of the exceptional flood event of July 2021 in central Europe—part 2: historical context and relation to climate change. Nat Hazards Earth Syst Sci 23:1287–1311. https://doi.org/10.5194/nhess-23-1287-2023
108. Völker C, Friedrich T, Kleespies MW, Marg O, Schiwy S (2023) "The toxic substance has killed all ducks": framing of chemical risks related to the 2021 summer flood in German news media. Environ Sci Eur. https://doi.org/10.1186/s12302-023-00789-2
109. Schwanen CA, Müller J, Schulte P, Schwarzbauer J (2023) Distribution, remobilization and accumulation of organic contaminants by flood events in a meso-scaled catchment system. Environ Sci Eur. https://doi.org/10.1186/s12302-023-00717-4
110. Weber A, Wolf S, Becker N, Märker-Neuhaus L, Bellanova P, Brüll C et al (2023) The risk may not be limited to flooding: polluted flood sediments pose a human health threat to the unaware public. Environ Sci Eur. https://doi.org/10.1186/s12302-023-00765-w
111. Lynch S, Batty L, Byrne P (2014) Environmental risk of metal mining contaminated river bank sediment at redox-transitional zones. Minerals 4:52–73. https://doi.org/10.3390/min4010052
112. Domínguez MT, Alegre JM, Madejón P, Madejón E, Burgos P, Cabrera F et al (2016) River banks and channels as hotspots of soil pollution after large-scale remediation of a river basin. Geoderma 261:133–140. https://doi.org/10.1016/j.geoderma.2015.07.008
113. Ciszewski D (1998) Channel processes as a factor controlling accumulation of heavy metals in river bottom sediments: consequences for pollution monitoring (Upper Silesia, Poland). Environ Geol 36:45–54. https://doi.org/10.1007/s002540050319
114. SPECTRO (2007) Analysis of trace elements in geological materials, soils and sludges prepared as pressed pellets.
115. Blott SJ, Pye K (2001) GRADISTAT: a grain size distribution and statistics package for the analysis of unconsolidated sediments. Earth Surf Process Landf 26:1237–1248. https://doi.org/10.1002/esp.261
116. DIN ISO 11277 Soil quality: determination of particle size distribution in mineral soil material—method by sieving and sedimentation 2002.
117. Özer M, Orhan M, Isik NS (2010) Effect of particle optical properties on size distribution of soils obtained by laser diffraction. Environ Eng Geosci 16:163–173. https://doi.org/10.2113/gseegeosci.16.2.163
118. Schulte P, Lehmkuhl F, Steininger F, Loibl D, Lockot G, Protze J et al (2016) Influence of HCl pretreatment and organo-mineral complexes on laser diffraction measurement of loess–paleosol-sequences. CATENA 137:392–405. https://doi.org/10.1016/j.catena.2015.10.015
119. ISO 13320 Particle size analysis —Laser Diffraction Methods: part 1: general principles, Annex A: theoretical background of laser diffraction 2009.
120. Rose AW, Dahlberg EC, Keith ML (1970) A multiple regression technique for adjusting background values in stream sediment geochemistry. Econ Geol 65:156–165. https://doi.org/10.2113/gsecongeo.65.2.156
121. Tapia J, Audry S, Townley B, Duprey JL (2012) Geochemical background, baseline and origin of contaminants from sediments in the mining-impacted Altiplano and Eastern Cordillera of Oruro, Bolivia. GEEA 12:3–20. https://doi.org/10.1144/1467-7873/10-RA-049
122. Salomão GN, Dall' Agnol R, Sahoo PK, Angélica RS, de MedeirosFilho CA, De Ferreira JS et al (2020) Geochemical mapping in stream sediments of the Carajás Mineral Province: Background values for the Itacaiúnas River watershed Brazi. Appl Geochem. https://doi.org/10.1016/j.apgeochem.2020.104608
123. Dominech S, Albanese S, Guarino A, Yang S (2022) Assessment on the source of geochemical anomalies in the sediments of the Changjiang river (China), using a modified enrichment factor based on multivariate statistical analyses. Environ Pollut 313:120126. https://doi.org/10.1016/j.envpol.2022.120126
124. Matschullat J, Ottenstein R, Reimann C (2000) Geochemical background—can we calculate it? Environ Geol 39:990–1000. https://doi.org/10.1007/s002549900084
125. Salminen R, Gregorauskien V (2000) Considerations regarding the definition of a geochemical baseline of elements in the surficial materials in areas differing in basic geology. Appl Geochem 15:647–653
126. Reimann C, Filzmoser P, Garrett RG (2005) Background and threshold: critical comparison of methods of determination. Sci Total Environ 346:1–16. https://doi.org/10.1016/j.scitotenv.2004.11.023
127. Adánez Sanjuán P, Ortega M, Llamas Borrajo JF, Locutura Rupérez J, García Cortés Á (2018) Statistical evaluation of the geochemical variability in overbank sediments in Spain. Environ Sci Pollut Res Int 25:29468–29480. https://doi.org/10.1007/s11356-018-2853-x
128. Gloaguen TV, Motta PNSD, Couto CF (2021) A grain-size correction for metal pollution indexes in river sediments. Int J Sedim Res 36:362–372. https://doi.org/10.1016/j.ijsrc.2020.10.005
129. Matys Grygar T (2020). Comments on "Evaluation of potentially toxic element contamination in the riparian zone of the River Sava" by

Pavlović et al. (2019). CATENA. 185:104032. doi:https://doi.org/10.1016/j.catena.2019.04.012.
130. Shotyk W, Weiss D, Appleby PG, Cheburkin AK, Gloor RF, Kramers JD et al (1998) History of atmospheric lead deposition since 12,370 (14)C yr BP from a peat bog, jura mountains, Switzerland. Science 281:1635–1640. https://doi.org/10.1126/science.281.5383.1635
131. Reimann C, Filzmoser P (2000) Normal and lognormal data distribution in geochemistry: death of a myth. consequences for the statistical treatment of geochemical and environmental data. Environ Geol 39:1001–1014. https://doi.org/10.1007/s002549900081
132. Tauler R, Paatero P, Henry RC, Spiegelman C, Park ES, Poirot RL et al (2008) Chapter fiveteen identification, resolution and apportionment of contamination sources. In: Tauler R, Paatero P, Henry RC, Spiegelman C, Park ES, Poirot RL (eds) Environmental modelling, software and decision support. Elsevier, Amsterdam, pp 269–284
133. Paatero P, Tapper U (1993) Analysis of different modes of factor analysis as least squares fit problems. Chemom Intell Lab Syst 18:183–194. https://doi.org/10.1016/0169-7439(93)80055-M
134. Paatero P, Hopke PK (2003) Discarding or downweighting high-noise variables in factor analytic models. Anal Chim Acta 490:277–289. https://doi.org/10.1016/S0003-2670(02)01643-4
135. Anttila P, Paatero P, Tapper U, Jarvinen O (1995) Source identification of bulk wet deposition in Finland by positive matrix factorization. Atmos Environ 29:1705–1718. https://doi.org/10.1016/1352-2310(94)00367-T
136. Esser V, Buchty-Lemke M, Schulte P, Podzun LS, Lehmkuhl F (2020) Signatures of recent pollution profiles in comparable central European rivers—examples from the international River Basin district Meuse. CATENA 193:104646. https://doi.org/10.1016/j.catena.2020.104646
137. Brown SG, Eberly S, Paatero P, Norris GA (2015) Methods for estimating uncertainty in PMF solutions: examples with ambient air and water quality data and guidance on reporting PMF results. Sci Total Environ 518–519:626–635. https://doi.org/10.1016/j.scitotenv.2015.01.022
138. Paatero P, Eberly S, Brown SG, Norris GA (2014) Methods for estimating uncertainty in factor analytic solutions. Atmos Meas Tech 7:781–797. https://doi.org/10.5194/amt-7-781-2014
139. Habre R, Coull B, Koutrakis P (2011) Impact of source collinearity in simulated PM2.5 data on the PMF receptor model solution. Atmos Environ 45:6938–6946. https://doi.org/10.1016/j.atmosenv.2011.09.034
140. Paatero P, Hopke P, Begum B, Biswas S (2005) A graphical diagnostic method for assessing the rotation in factor analytical models of atmospheric pollution. Atmos Environ 39:193–201. https://doi.org/10.1016/j.atmosenv.2004.08.018
141. Chen L, Wang G, Wu S, Xia Z, Cui Z, Wang C, Zhou S (2019) Heavy metals in agricultural soils of the lihe river watershed, east China spatial distribution, ecological risk, and pollution source. Int J Environ Res Public Health. https://doi.org/10.3390/ijerph16122094
142. Comero S, Vaccaro S, Locoro G, de Capitani L, Gawlik BM (2014) Characterization of the Danube River sediments using the PMF multivariate approach. Chemosphere 95:329–335. https://doi.org/10.1016/j.chemosphere.2013.09.028
143. Chen S, Wu P, Zha X, Zhou B, Liu J, Long E (2023) Arsenic and heavy metals in sediments affected by typical gold mining areas in southwest China accumulation, sources and ecological risks. Int J Environ Res Public Health. https://doi.org/10.3390/ijerph20021432
144. Huang S, Conte MH (2009) Source/process apportionment of major and trace elements in sinking particles in the Sargasso sea. Geochim Cosmochim Acta 73:65–90. https://doi.org/10.1016/j.gca.2008.08.023
145. Grunsky EC, Drew LJ, Sutphin DM (2009) Process recognition in multi-element soil and stream-sediment geochemical data. Appl Geochem 24:1602–1616. https://doi.org/10.1016/j.apgeochem.2009.04.024
146. Agyeman PC, Ahado SK, John K, Kebonye NM, Vašát R, Borůvka L et al (2021) Health risk assessment and the application of CF-PMF: a pollution assessment–based receptor model in an urban soil. J Soils Sediment 21:3117–3136. https://doi.org/10.1007/s11368-021-02988-x
147. Amjadian K, Pirouei M, Rastegari Mehr M, Shakeri A, Khurshid Rasool S, Ibrahim Haji D (2018) Contamination, health risk, mineralogical and morphological status of street dusts- case study: Erbil metropolis, kurdistan region-Iraq. Environ Pollut 243:1568–1578. https://doi.org/10.1016/j.envpol.2018.09.116
148. Chen R, Chen H, Song L, Yao Z, Meng F, Teng Y (2019) Characterization and source apportionment of heavy metals in the sediments of Lake Tai (China) and its surrounding soils. Sci Total Environ 694:133819. https://doi.org/10.1016/j.scitotenv.2019.133819
149. Chen Z, Shi Z, Ni S, Cheng L (2022) Characteristics of soil pollution and element migration associated with the use of coal in Hutou village, Yunnan province. China Ecol Indic 139:108976. https://doi.org/10.1016/j.ecolind.2022.108976
150. Du H, Wang J, Wang Y, Yao Y, Liu X, Zhou Y (2023) Contamination characteristics, source analysis, and spatial prediction of soil heavy metal concentrations on the Qinghai-Tibet Plateau. J Soils Sediments. https://doi.org/10.1007/s11368-023-03462-6
151. Wang L, Han X, Ding S, Liang T, Zhang Y, Xiao J et al (2019) Combining multiple methods for provenance discrimination based on rare earth element geochemistry in lake sediment. Sci Total Environ 672:264–274. https://doi.org/10.1016/j.scitotenv.2019.03.484
152. Balan E, Trocellier P, Jupille J, Fritsch E, Muller J-P, Calas G (2001) Surface chemistry of weathered zircons. Chem Geol 181:13–22. https://doi.org/10.1016/S0009-2541(01)00271-6
153. Garçon M, Chauvel C, France-Lanord C, Huyghe P, Lavé J (2013) Continental sedimentary processes decouple Nd and Hf isotopes. Geochim Cosmochim Acta 121:177–195. https://doi.org/10.1016/j.gca.2013.07.027
154. Komar PD (2007) Chapter 1 the entrainment, transport and sorting of heavy minerals by waves and currents. In: Komar PD (ed) Heavy minerals in use. Elsevier, Amsterdam
155. Tarvainen T, Salminen R, de Vos W (2006) Geochemical atlas of Europe background information, methodology and maps. Geological Survey of Finland, Espoo
156. Mohanty S, Papadopoulos A, Petrelli M, Papadopoulou L, Sengupta D (2023) geochemical studies of detrital zircon grains from the river banks and beach placers of coastal Odisha. India Minerals 13:192. https://doi.org/10.3390/min13020192
157. Vos WD, Travainen T, Reeder S (2006) Geochemical atlas of Europe part 2 interpretation of geochemical maps, additional tables, figures, maps and related publications. Geological Survey of Finland, Espoo
158. Vos WD, Batista MJ, Pirc S, Oconnor PJ, Demetriades A, Tarvainen T et al (2006) Distribution of elements in stream sediment. In: Vos WD, Travainen T, Reeder S (eds) Geochemical atlas of Europe. Part 2: Interpretation of geochemical maps, additional tables, figures, maps and related publications. Geological Survey of Finland, Espoo, pp 37–40
159. Lupker M, France-Lanord C, Lavé J, Bouchez J, Galy V, Métivier F et al (2011) A rouse-based method to integrate the chemical composition of river sediments: application to the Ganga basin. J Geophys Res. https://doi.org/10.1029/2010JF001947
160. Felix-Henningsen P, Spies E-D, Zakosek H (1991) Genese und stratigraphie periglazialer deckschichten auf der hochfläche des ost-hunsrücks (Rheinisches Schiefergebirge). Quat Sci J. https://doi.org/10.23689/fidgeo-1595
161. van Andel TH (1950). Provenance, transport and deposition of Rhine sediments: a heavy mineral study on river sands from the drainage area of the Rhine. Dissertation, Groningen.
162. Janus U Löss der südlichen Niederrheinischen Bucht, Köln. 1988
163. Bhuiyan MAH, Dampare SB, Islam MA, Suzuki S (2015) Source apportionment and pollution evaluation of heavy metals in water and sediments of Buriganga River, Bangladesh, using multivariate analysis and pollution evaluation indices. Environ Monit Assess 187:4075. https://doi.org/10.1007/s10661-014-4075-0
164. Li T, Sun G, Yang C, Liang K, Ma S, Huang L, Luo W (2019) Source apportionment and source-to-sink transport of major and trace elements in coastal sediments: combining positive matrix factorization and sediment trend analysis. Sci Total Environ 651:344–356. https://doi.org/10.1016/j.scitotenv.2018.09.198
165. Ewers U, Brockhaus A, Winneke G, Freier I, Jermann E, Krämer U (1982) Lead in deciduous teeth of children living in a non-ferrous smelter area and a rural area of the FRG. Int Arch Occup Environ Health 50:139–151. https://doi.org/10.1007/BF00378076
166. Ewers U, Turfeld M, Freier I, Brockhaus A (1996) Blei–und cadmiumbelastung zähne als indikatoren der blei–und cadmiumbelastung des menschen. UWSF–Z Umweltchem Ökotox 8:312–316. https://doi.org/10.1007/BF02945901
167. Sun R, Gao Y, Xu J, Yang Y, Zhang Y (2021) Contamination features and source apportionment of heavy metals in the river sediments around

a lead-zinc mine: a case study in Danzhai, Guizhou, China. J Chem 2021:1–11. https://doi.org/10.1155/2021/9946026
168. Zuliani T, Vidmar J, Ščančar J, Kolarević MK, Kolarević S, Paunović M, Milačič R (2022) Transport of potentially toxic elements in solid particulate matter during flash flood events in upper and lower stretch of the Sava River. Water 14:1213. https://doi.org/10.3390/w14081213
169. Kourgia PM, Argyraki A, Paraskevopoulou V, Botsou F, Kelepertzis E, Dassenakis M (2022) Environmental fate of trace elements in depositional sediments after flashflood events: the case of mandra town in Greece. Sustainability 14:2448. https://doi.org/10.3390/su14042448
170. Aguilar G, Valdés A, Cabré A, Galdames F (2021) Flash floods controlling Cu, Pb, As and Hg variations in fluvial sediments of a river impacted by metal mining in the Atacama Desert. J S Am Earth Sci 109:103290. https://doi.org/10.1016/j.jsames.2021.103290
171. Resongles E, Casiot C, Freydier R, Dezileau L, Viers J, Elbaz-Poulichet F (2014) Persisting impact of historical mining activity to metal (Pb, Zn, Cd, Tl, Hg) and metalloid (As, Sb) enrichment in sediments of the Gardon River, Southern France. Sci Total Environ 481:509–521. https://doi.org/10.1016/j.scitotenv.2014.02.078
172. Kabata-Pendias A (2010) Trace elements in soils and plants. CRC Press, Boca raton
173. Haddadchi A, Rose CW (2022) A physically based model of deposition, re-entrainment, and transport of fine sediment in gravel-bed rivers. Water Resour Res. https://doi.org/10.1029/2021WR031782
174. Bradley SB (1984) Flood effects on the transport of heavy metals. Int J Environ Stud 22:225–230. https://doi.org/10.1080/00207238408710121
175. Blöthe JH, Hoffmann T (2022) Spatio-temporal differences dominate suspended sediment dynamics in medium-sized catchments in central Germany. Geomorphology 418:108462. https://doi.org/10.1016/j.geomorph.2022.108462
176. Naden PS (2010) The fine-sediment cascade. In: Burt T, Allison RJ (eds) Sediment cascades an integrated approach. Wiley, Hoboken, pp 271–305
177. Wharton G, Mohajeri SH, Righetti M (2017) The pernicious problem of streambed colmation: a multi-disciplinary reflection on the mechanisms, causes, impacts, and management challenges. WIREs Water. https://doi.org/10.1002/wat2.1231
178. Lehmkuhl F, Weber A, Esser V, Schulte P, Wolf S, Schrumpf H (2022) Fluviale morphodynamik und sedimentkontamination bei extremereignissen: das juli-hochwasser 2021 im inde-einzugsgebiet (Nordrhein-Westfalen). Korrespondenz Wasserwirtschaft 2:422–427
179. Macklin MG, Klimek K (1992) Dispersal, storage and transformation of metalcontaminated alluvium in the upper vistula basin, southwest Poland. Appl Geogr 12:7–30. https://doi.org/10.1016/0143-6228(92)90023-G
180. Dennis IA, Coulthard TJ, Brewer P, Macklin MG (2009) The role of floodplains in attenuating contaminated sediment fluxes in formerly mined drainage basins. Earth Surf Process Landf 34:453–466. https://doi.org/10.1002/esp.1762
181. Lecce SA, Pavlowsky RT (1997) Storage of mining-related zinc in floodplain sediments, Blue River, Wisconsin. Phys Geogr 18:424–439. https://doi.org/10.1080/02723646.1997.10642628
182. Lecce SA, Pavlowsky RT (2014) Floodplain storage of sediment contaminated by mercury and copper from historic gold mining at gold hill, North Carolina, USA. Geomorphology 206:122–132. https://doi.org/10.1016/j.geomorph.2013.10.004
183. Kincey M, Warburton J, Brewer P (2018) Contaminated sediment flux from eroding abandoned historical metal mines: spatial and temporal variability in geomorphological drivers. Geomorphology 319:199–215. https://doi.org/10.1016/j.geomorph.2018.07.026
184. Gozzard E, Mayes WM, Potter HAB, Jarvis AP (2011) Seasonal and spatial variation of diffuse (non-point) source zinc pollution in a historically metal mined river catchment, UK. Environ Pollut 159:3113–3122. https://doi.org/10.1016/j.envpol.2011.02.010
185. Macklin MG, Brewer PA, Hudson-Edwards KA, Bird G, Coulthard TJ, Dennis IA et al (2006) A geomorphological approach to the management of rivers contaminated by metal mining. Geomorphology 79:423–447. https://doi.org/10.1016/j.geomorph.2006.06.024
186. Ayari J, Barbieri M, Agnan Y, Sellami A, Braham A, Dhaha F, Charef A (2021) Trace element contamination in the mine-affected stream sediments of Oued Rarai in north-western Tunisia: a river basin scale assessment. Environ Geochem Health 43:4027–4042. https://doi.org/10.1007/s10653-021-00887-1
187. Marchi L, Borga M, Preciso E, Gaume E (2010) Characterisation of selected extreme flash floods in Europe and implications for flood risk management. J Hydrol 394:118–133. https://doi.org/10.1016/j.jhydrol.2010.07.017
188. Schröter K, Kunz M, Elmer F, Mühr B, Merz B (2015) What made the june 2013 flood in Germany an exceptional event? a hydro-meteorological evaluation. Hydrol Earth Syst Sci 19:309–327. https://doi.org/10.5194/hess-19-309-2015
189. Du Laing G, Rinklebe J, Vandecasteele B, Meers E, Tack FMG (2009) Trace metal behaviour in estuarine and riverine floodplain soils and sediments: a review. Sci Total Environ 407:3972–3985. https://doi.org/10.1016/j.scitotenv.2008.07.025
190. Hahn J, Opp C, Zitzer N, Laufenberg G (2016) Impacts of river impoundment on dissolved heavy metals in floodplain soils of the Lahn River (Germany). Environ Earth Sci. https://doi.org/10.1007/s12665-016-5950-5
191. Heller K, Kleber A (2016) Hillslope runoff generation influenced by layered subsurface in a headwater catchment in Ore Mountains. Environ Earth Sci, Germany. https://doi.org/10.1007/s12665-016-5750-y
192. Hawkes HE (1976) The downstream dilution of stream sediment anomalies. J Geochem Explor 6:345–358. https://doi.org/10.1016/0375-6742(76)90023-6
193. Schulte P, Hamacher H, Lehmkuhl F, Esser V (2022) Initial soil formation in an artificial river valley—interplay of anthropogenic landscape shaping and fluvial dynamics. Geomorphology 398:108064. https://doi.org/10.1016/j.geomorph.2021.108064
194. Maaß A-L, Schüttrumpf H (2019) Reactivation of floodplains in river restorations: long-term implications on the mobility of floodplain sediment deposits. Water Resour Res 55:8178–8196. https://doi.org/10.1029/2019WR024983
195. Schulte P, Weber A, Keßels J, Lehmkuhl F, Schüttrumpf H, Esser V, Wolf S (2024) Morphodynamics and heavy metal accumulation in an artificially built near-natural river (Inde, Germany). J Sediment Environ 9:117–133. https://doi.org/10.1007/s43217-023-00160-8
196. Collenteur RA, de Moel H, Jongman B, Di Baldassarre G (2015) The failed-levee effect: do societies learn from flood disasters? Nat Hazards 76:373–388. https://doi.org/10.1007/s11069-014-1496-6
197. Fekete A, Sandholz S (2021) Here comes the flood, but not failure? Lessons to learn after the heavy rain and pluvial floods in Germany 2021. Water 13:3016. https://doi.org/10.3390/w13213016
198. Špitalar M, Gourley JJ, Lutoff C, Kirstetter P-E, Brilly M, Carr N (2014) Analysis of flash flood parameters and human impacts in the US from 2006 to 2012. J Hydrol 519:863–870. https://doi.org/10.1016/j.jhydrol.2014.07.004
199. Proshad R, Kormoker T, Abdullah Al M, Islam MS, Khadka S, Idris AM (2022) Receptor model-based source apportionment and ecological risk of metals in sediments of an urban river in Bangladesh. J Hazard Mater 423:127030. https://doi.org/10.1016/j.jhazmat.2021.127030
200. Chen X, Lei M, Zhang S, Zhang D, Guo G, Zhao X (2022) Apportionment and spatial pattern analysis of soil heavy metal pollution sources related to industries of concern in a county in southwestern China. Int J Environ Res Public Health. https://doi.org/10.3390/ijerph19127421
201. Rugi F, Udisti R, Becagli S, Frosini D, Giorgetti G, Kuhn G et al (2015) One-million year rare earth element stratigraphies along an antarctic marine sediment core. Microchem J 122:164–171. https://doi.org/10.1016/j.microc.2015.04.020
202. Karakas F, Imamoglu I, Gedik K (2017) Positive matrix factorization dynamics in fingerprinting: a comparative study of PMF2 and EPA-PMF3 for source apportionment of sediment polychlorinated biphenyls. Environ Pollut 220:20–28. https://doi.org/10.1016/j.envpol.2016.07.066
203. Shi G-L, Chen H, Tian Y-Z, Song D-L, Zhou L-D, Chen F et al (2016) Effect of uncertainty on source contributions from the positive matrix factorization model for a source apportionment study. Aerosol Air Qual Res 16:1665–1674. https://doi.org/10.4209/aaqr.2015.12.0678
204. Hemann JG, Brinkman GL, Dutton SJ, Hannigan MP, Milford JB, Miller SL (2009) Assessing positive matrix factorization model fit: a new method to estimate uncertainty and bias in factor contributions at the measurement time scale. Atmos Chem Phys 9:497–513. https://doi.org/10.5194/acp-9-497-2009

205. Salau JS, Tauler R, Bayona JM, Tolosa I (1997) Input characterization of sedimentary organic contaminants and molecular markers in the northwestern mediterranean sea by exploratory data analysis. Environ Sci Technol 31:3482–3490. https://doi.org/10.1021/es970231e
206. Hopke PK (2003) Recent developments in receptor modeling. J Chemometrics 17:255–265. https://doi.org/10.1002/cem.796
207. Sun X, Wang H, Guo Z, Lu P, Song F, Liu L et al (2020) Positive matrix factorization on source apportionment for typical pollutants in different environmental media: a review. Environ Sci Process Impacts 22:239–255. https://doi.org/10.1039/C9EM00529C
208. Henry RC, Christensen ER (2010) Selecting an appropriate multivariate source apportionment model result. Environ Sci Technol 44:2474–2481. https://doi.org/10.1021/es9018095

Publisher's Note